Desalination and Water Treatment
www.deswater.com

doi: 10.1080/19443994.2013.870776

53 (2015) 1780–1804
February

Taylor & Francis
Taylor & Francis Group

Closed circuit desalination series no-12: the use of 4, 5 and 6 element modules with the BWRO-CCD technology for high recovery, low energy and reduced fouling applications

Avi Efraty

Desalitech Ltd, P.O. Box 132, Har Adar 90836, Israel
Email: avi@desalitech.com

Received 29 June 2013; Accepted 17 October 2013

ABSTRACT

The newly emerging closed circuit desalination (CCD) technologies of high recovery and low energy for seawater (SWRO-CCD) and brackish water (BWRO-CCD) have been demonstrated thus far with short modules comprising one to four elements (MEn; $n = 1$–4). The present study explores the plausible application of longer modules of five to six elements each (ME5 and ME6) in the context of the BWRO-CCD technology on the basis of theoretical model simulations with emphasis on recovery, energy consumption, permeates quality and membrane fouling aspects. The plausibility of the ME4 (MR = 40–50%), ME5 (MR = 40–60%) and ME6 (MR = 40–65%) modules in the cited Module Recovery (MR) ranges (in parentheses) for BWRO-CCD application has been confirmed by IMS Design results on such modules with ESPA2-MAX elements using 2,500 ppm NaCl feed at flux of 24.5 lmh. In order to establish the relationships between conventional BWRO and BWRO-CCD which operates on the basis of different principles, a comprehensive theoretical model analysis was performed on the 4ME6 + 2ME5 + ME6 conventional system compared with the 7ME6 BWRO-CCD unit design of the same number of modules and elements (ESPA2-MAX) under similar and different flux conditions for recovery of ~90% using the same feed source (2,500 ppm NaCl) and identical theoretical equations to generate the compared data. The noteworthy conclusions reached from the results of the comparative theoretical study are as follows: (1) BWRO-CCD may reach any desired high recovery made possible by the composition and quality of the source without need of staged pressure vessels and booster pumps and with greater facility and flexibility compared with conventional techniques. (2) The energy consumption of BWRO-CCD is considerably lower compared with that of conventional techniques under same flux conditions, especially in the 80–90% recovery range, without any need for energy recovery. (3) The quality of BWRO-CCD permeates in the 80–90% recovery range is somewhat inferior to that of conventional techniques under the same flux conditions. (4) BWRO-CCD flux increase of ~25% compared with that of conventional techniques will lead to similar quality permeates in the 80–90% recovery range with lower energy consumption by the former despite the flux increase. (5) Convention multi-stage BWRO techniques require high MR in the first stage (up to ~65%) in order to reach ultimate high process recovery and this implies increased probability of fouling and scaling of tail elements due to decreased average cross-flow; whereas, MR in BWRO-CCD is independent of sequence recovery and this implies the ability to select MR of desired cross-flow to minimize fouling and scaling effects.

Keywords: Closed circuit desalination; CCD; High recovery; High flux; Low energy; Reduced fouling; Brackish water desalination; Staged BWRO system designs

1. Introduction

Conventional single pass RO desalination of seawater (SWRO) [1–5] normally proceeds with 45–50% recovery using modules of 7–8 elements each (ME7 or ME8) with energy recovery means (e.g. DWEER, PX, PELTON, etc.) in order to save some/most of the energy stored in the disposed brine. By comparison, conventional RO desalination of brackish water (BWRO) [5–9] commonly utilizes modules of 6 elements each (ME6) and proceeds with 75–90% recovery using multi-stage (2 or 3 stages) processes with staged pressure vessels and inter-stage booster or turbo-charger pumps. The meaning of energy recovery from brine in BWRO declines with increased recovery for obvious reasons and practiced mainly in the context of the 2-stage BWRO process for 75–85% recovery with an inter-stage turbo-charger booster driven by pressurized brine effluent. Desalination of brackish water with recovery greater than 85% normally proceeds with three stage systems with or without inter-stage boosters and without ER means. The most common problems encountered with conventional BWRO techniques relate to membranes' fouling due to particulate matter in the feed and/or bacteria growth on membrane surfaces (bio-fouling) and/or scaling of low solubility precipitates (e.g. $CaCO_3$, $CaSO_4$, $BaSO_4$, silicates, etc.) [9] in high recovery processes. In simple terms, the conditions of specific BWRO desalination applications require adjustments to meet the nature of each source and its composition in order to minimize adverse operational effects.

Several recent publications during the past year and half describe the newly emerging RO technologies of closed circuit desalination (CCD) by means of consecutive sequential batch processes and their applications for seawater desalination (SWRO-CCD) [10–14] and for brackish water desalination (BWRO-CCD) [15–19]. The CCD technologies are performed under fixed flow and variable pressure conditions with high recovery determined only by the maximum applied pressure of operation irrespective of the number of elements per module, low energy of near theoretical minimum without need of energy recovery means and reduced fouling and bio-fouling characteristics. The reported data thus far on CCD processes pertains to the performance of units comprising modules of 1–4 elements (MEn: $n = 1$–4), originated from theory [20,21] and confirmed by consistent experimental results. The current paper describes the plausible extension of the BWRO-CCD technology to include modules of 5 and 6 elements and provides a comparative theoretical model analysis between conventional BWRO and BWRO-CCD in the context of high recovery low energy applications.

2. Overview—conventional BWRO vs. BWRO-CCD

High recovery (>87.5%) desalination of brackish water by conventional BWRO techniques with six elements modules normally requires a three stage process with staged pressure vessels and inter-stage booster pumps in order to be effective. The schematic design of a typical conventional BWRO system for high recovery desalination in Fig. 1 comprises identical modules, each of six elements, with four modules in first stage (4ME6), two in second stage (2ME6) and one in the third stage (ME6) with inter-stage booster pumps (BP-1 and PB-2), whereby most production(60–65%) takes place in the first stage. If the pressure and flow conditions of the first stage are tuned for 50% recovery and the booster pumps enable the same flow conditions also in the second and third stages by compensating for the increased of osmotic pressures and Δp, this will lead to the cumulative recovery of 50.0, 75.0 and 87.5% after the first, second and third stage through a line of 6, 12 and 18 elements, respectively.

The equivalent design of the conventional system (Fig. 1) in terms of the same number of modules and elements by the recently reported [15–19] BWRO-CCD technology is depicted schematically in Fig. 2 (NMEn: $N = 7$ and $n = 6$); wherein, the respective inlets and outlets of modules are connected in parallel to the same closed circuit, the desired cross flow is created by a circulation pump with variable frequency drive control means (CP-vfd) and the desired pressurized feed flow at inlet to unit supplied by a high pressure pump with variable frequency drive control means (HP-vfd). Other features in Fig. 2 include an actuated valve means (AV) extending from the closed circuit, a check valve (One Way Valve—OWV) means in the closed circuit down stream form the AV extension as well as monitoring means (not shown) of flow,

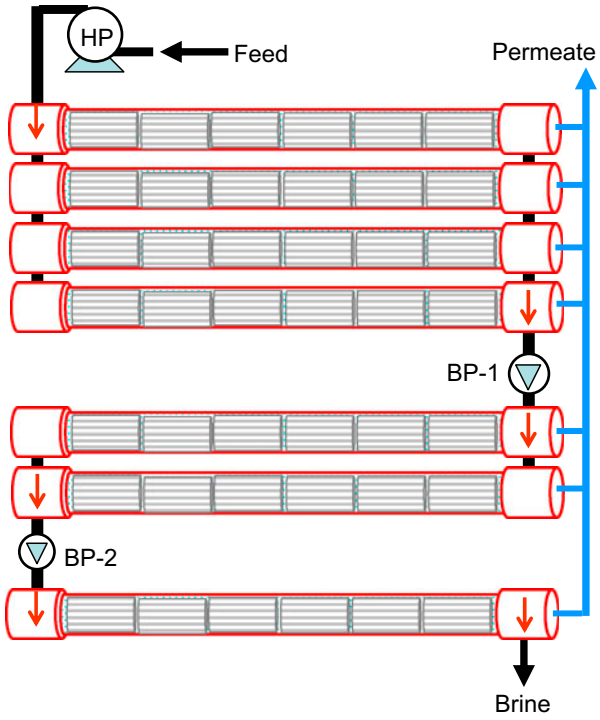

Fig. 1. A schematic design of a minimum size 3 stage (4ME6:2ME6:ME6) conventional BWRO system with high pressure pump (HP) and two inter-stage booster pumps (BP-1 and BP-2) for high recovery (≥87.5%) desalination of brackish water sources.

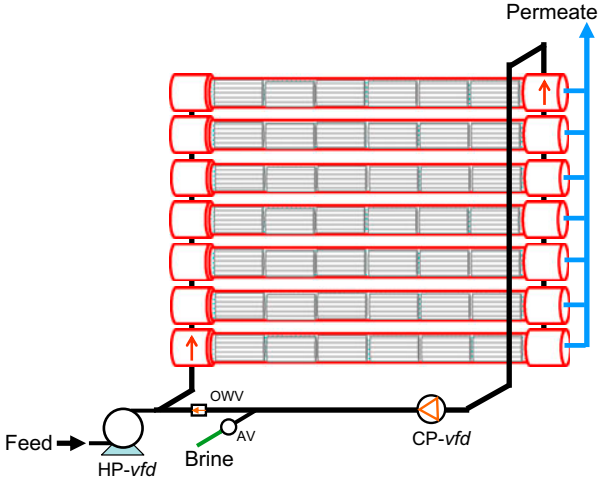

Fig. 2. A schematic design of continuously flow staged and pressure boosted 7ME6 BWRO-CCD unit with high pressure pump (HP-vfd), circulation pump (CP-vfd), actuated 2-way valve means (AV) and check valve (OWV—one way valve) means for high recovery (>87.5%) desalination of Brackish Water.

pressure, electric conductivity and temperature as appropriate for the control of the unit and/or the monitoring of its performance. The reported [15–19] actuation of the BWRO-CCD unit proceeds by a two-step consecutive sequential process under fixed flow and variable pressure conditions in closed circuit (CCD) with brief intervals of open circuit plug flow desalination (PFD) steps between sequential CCD cycles for the replacement brine by fresh feed at the desired recovery level without stopping desalination. The sequential CCD cycles are performed with selected set-points of pressurized feed flow (Q_f) and cross-flow (Q_{CP}) with module recovery (MR) expressed by $MR = Q_p/(Q_f + Q_{CP}) \times 100 = Q_f/(Q_f + Q_{CP}) \times 100$; wherein, feed flow ($Q_f$) and permeate flow ($Q_p$) are the same ($Q_p = Q_f$). A maximum CCD applied pressure set-point manifests the desired recovery of the system and attainment of this pressure triggers the CCD → PFD shift by the opening of AV and stopping of CP. The brine volume removed during PFD is monitored by the flow/volume metre downstream from CP and the match between the replaced brine volume and the fixed intrinsic volume of the closed circuit triggers the PFD → CCD shift with the closure of AV and resumption of CP. The BWRO-CCD system under review can be optimized, including online, by an infinite number of set-points combinations since said set-points of Q_f, Q_{CP} and maximum CCD applied pressure are independent of each other and this implies a highly flexible technology.

Compared with conventional BWRO, BWRO-CCD is based on a conceptually differ technology from the stand points of engineering and operational principles and some noteworthy distinctions between the technologies are outlined next. In contrast with conventional techniques, the staged flow and pressure-boosted BWRO-CCD process does not required staged pressure vessels and booster pumps and may apply to any NMEn design even of a single element module ($N = n = 1$). The modules in the design will perform uniformly the same during the entire CCD sequences with period time of each sequence determined by the number of CCD cycles required to reach the desired recovery manifested only by the selected set-point of maximum applied pressure and this irrespective of the number of elements per module and/or the number of modules per design. The recycled concentrate during the CCD sequences is diluted with fresh feed at inlets to modules, since flow at inlets to modules combines Q_f and Q_{CP} and this dictates the concentration relationships between modules inlets (C_i) and outlets (C_o) of $C_i = C_o \times Q_{CP}/(Q_f + Q_{CP})$ or $C_o/C_i = 1 + Q_f/Q_{CP}$. The dilution effect implies that the probability of scaling is pushed towards the very last CCD cycle in

the sequential process and if this flexibly controlled technology is sufficiently optimized, high recovery is attainable with decreased probability of fouling. The simple BWRO-CCD modular designs of the type of NMEn and their effective control means of pressurized feed flow (Q_f), permeate flow (Q_p) or flux, cross-flow (Q_{CP}) and recovery independent of any of the flow rates, provide a unique desalination technology for high recovery and low energy desalination under reduced fouling characteristics for wide range diverse applications.

3. BWRO-CCD MEn(n = 4–6) module performance evaluation

The performance of the repeated identical CCD cycles during the consecutive sequential process in BWRO-CCD apparatus of MEn module designs can be evaluated by means of computer design programs of membrane producers and this approach is illustrated next for the MEn (E = ESPA2-MAX, n = 4–6) modules in Table 1 by means of the IMS Design program. The data in Table 1 pertains to fixed flux (24.5 lmh) operation of modules with 4, 5 and 6 elements in the MR range 40–65% starting with feed of 2,500 ppm NaCl (pH = 7.0 and 25˚C). The data in the table is confined to the allowed operation conditions of the program (beta < 1.2; module inlet feed < 17.1 m^3/h, etc.) and in case of NaCl feed the limiting flux it 46.35 lmh that of the ESPA2-MAX element under test conditions. The MR limits of 60% for ME5 and 50% for ME4 modules are defined by the program. The calculated terms on right-hand side of the table are derived from the IMS Design data and pertain to the average element recovery (Y_{av}) according to Eq. (1), the average concentration polarization factor (pf_{av}) according to Eq. (2), the recovery of the head and tail elements on the basis of the flux data and the pf of the head and tail elements on the basis of Eq. (2) wherein the recovery ratio of said elements used instead of Y_{av}. The coefficient $k = 0.375$ in Eq. (2) gave the best agreement with IMS Design data.

$$Y_{av} = 1 - (1 - MR/100)^{1/n} \quad (1)$$

$$pf_{av} = 100^{k*Y_{av}} \quad (2)$$

The data in Table 1 under identical average flux conditions suggests the plausibility of the module units ME6 (MR = 40–65%), ME5 (MR = 40–60%) and ME4 (MR = 40–50%) for BWRO-CCD applications in the specified (in parentheses) MR ranges without

Table 1
IMS design comparative performance data for MEn (E = ESPA2-MAX; n = 4–6) modules with 2,500 ppm NaCl feed under the specified flow and applied pressure conditions at fixed flux (24.5 lmh), pH = 7.0 and 25˚C without exceeding any of the computerized design program restrictions with regards to maximum beta (1.20) and flow conditions (e.g. 17.1 m^3/h maximum feed flow at inlet to module)

IMS design: ESPA2-MAX; 2,500 ppn NaCl; pH = 7.0; Temp.= 25˚													Calculated terms form IMS design data					
	Flow				Flux			Pressure					Average		Recovery		pf-element	
Module design	Perm. m^3/h	Feed m^3/h	Conc. m^3/h	Rec %	Averge lmh	Head lmh	Tail lmh	Head bar	Tail bar	Δp bar	pf beta factor	Perm. TDS ppm	Element Y_{av}	Module pf_{av}	Head %	Tail %	Head factor	Tail factor
ME6	6.0	15.0	9.0	40.0	24.5	33.7	16.1	8.9	6.1	2.80	1.07	32.9	8.2	1.07	9.2	6.8	1.08	1.06
ME6	6.0	13.3	7.3	45.0	24.5	33.1	16.4	8.7	6.5	2.20	1.08	35.2	9.5	1.09	10.1	8.4	1.09	1.07
ME6	6.0	12.0	6.0	50.0	24.5	32.8	16.3	8.7	6.8	1.90	1.10	38.1	10.9	1.10	11.2	10.0	1.10	1.09
ME6	6.0	10.9	4.9	55.0	24.5	32.9	15.9	8.7	7.2	1.50	1.12	41.7	12.5	1.11	12.3	11.7	1.11	1.11
ME6	6.0	10.0	4.0	60.0	24.5	33.4	15.0	8.8	7.5	1.30	1.14	46.2	14.2	1.13	13.6	13.3	1.12	1.12
ME6	6.0	9.2	3.2	65.0	24.5	34.2	13.6	8.9	7.9	1.00	1.15	51.7	16.1	1.15	15.1	14.7	1.14	1.13
ME5	5.0	12.5	7.5	40.0	24.5	31.1	18.1	8.3	6.5	1.80	1.09	32.3	9.7	1.09	10.2	9.0	1.09	1.08
ME5	5.0	11.1	6.1	45.0	24.5	30.8	18.1	8.3	6.8	1.50	1.11	45.5	11.3	1.10	11.3	10.8	1.10	1.10
ME5	5.0	10.0	5.0	50.0	24.5	31.0	17.8	8.3	7.1	1.20	1.13	37.3	12.9	1.12	12.6	12.7	1.12	1.12
ME5	5.0	9.1	4.1	55.0	24.5	31.3	17.1	8.3	7.4	0.90	1.15	40.8	14.8	1.14	14.0	14.6	1.13	1.13
ME5	5.0	8.3	3.3	60.0	24.5	31.9	16.1	8.5	7.7	0.80	1.18	45.3	16.7	1.16	15.6	16.5	1.14	1.15
ME4	4.0	10.0	6.0	40.0	24.5	29.0	19.7	7.9	6.8	1.10	1.10	31.7	12.0	1.11	11.8	11.8	1.11	1.11
ME4	4.0	8.9	4.9	45.0	24.5	29.2	19.5	7.9	7.1	0.80	1.10	33.8	13.9	1.13	13.4	14.0	1.12	1.13
ME4	4.0	8.0	4.0	50.0	24.5	29.5	19.0	8.0	7.3	0.70	1.10	36.8	15.9	1.15	15.0	16.2	1.14	1.15

exceeding any of the performance limitations of such membranes according to their computerized design programs. The data in the table under review reveals the expected trend of increased MR concomitance with increased recovery of the average element, the head and the tail elements and their respective concentration polarization factors (beta). Comparing between the head and tail (in parentheses) element recovery of the different MEn ($n = 4$–6) configurations at the same MR reveals the increased order ME6 < ME5 < ME4 [e.g. MR = 40%: 9.2%(6.8%) < 10.2%(9.0%) < 11.8% (11.8%) and MR = 50%: 11.2%(10.0%) < 12.6% (12.7%) < 15.0%(16.5%)] and since increased MR implies lower cross-flow these results suggest the operational preference of lower MR for reduction of particulate matter fouling because higher cross-flow creates greater momentum vector for such particles in the direction of the cross-flow away from membrane surfaces. Permeates TDS are determined primarily as function flux, feed concentration and beta and therefore, should be similar at the same flux and MR irrespective of the module configuration with minor differences accounting to beta as evident by the results in the table [e.g. MR = 50%: ME6 (38.1 ppm; $pf_{av} = 1.10$); ME5 (37.3 ppm; $pf_{av} = 1.12$) and ME4 (36.8 ppm; $pf_{av} = 1.15$)]. The flux distribution span between head and tail elements of the MEn module configurations under the same average flux conditions reveals strong dependence on the number of elements per module (n) with little, if any, dependence on MR (e.g. ME6: 24.5 ± 9.0 lmh; ME5: 24.5 ± 7.0 lmh and ME4: 24.5 ± 5.0 lmh). The deviation of the head or tail elements flux from the average manifests the range of over and under average performance characteristics of said elements with greater deviation implying decreased performance uniformity within modules with front elements more prone to fouling and tail elements to scaling. Decreased performance uniformity of elements implies greater wear of front and tails elements, more frequent needs for CIP procedures and/or for replacement of old elements by new. In view of the aforementioned, the selection of the MEn module design in the context of BWRO-CCD should address the feed quality and its composition with shorter modules favoured for feed sources of increased fouling characteristics.

The preference of the ME4 module in BWRO-CCD applications of high performance uniformity with suggested low fouling–scaling characteristics prompted the IMS Design analysis this module with feed of 2,500 ppm NaCl and ESPA2-MAX elements in the MR range 35–50% under different CCD average flux of 24.5; 27.5; 30.6; 33.6 and 36.7 lmh with maximum head element flux of 43.0 lmh just below the test conditions value (46.35 lmh) and the results of this comparative study are summarized in Table 2. The results in the table under view reveal a small systematic rise in modules' flux difference (head less tail) of 9.7 < 10.3 < 11.2 < 12.5 < 12.9 lmh as function of the increased average operational flux 24.5 < 27.5 < 30.6 < 33.6 < 36.7 lmh, respectively. Moreover, variation of parameters induced by MR change of 35–50% are almost independent of the average flux as evident by the ranges of Y_{av}(10.2–15.5%) and pf_{av} (1.09–1.14) as well as by the equivalent ranges of the head and tail elements, wherein some minor variations are observed. Operating in the indicated average flux range 24.5–6.7 lmh with MR of 35–50% also imply according to Table 2 a similar respective head element recovery range [10.4–15.0% (beta: 1.09–1.13)] and tail element recovery range [9.8–17.0% (beta: 1.08–1.15)] only as function of MR and therefore, irrespective of the average flux of operation. In simple terms, the head and tail element recovery could be maintained at a desired level irrespective of flux by simple MR control. Accordingly, irrespective of the selected average flux of operation, the choice of MR should relate to the quality and composition of the feed source with lower MR, which manifests faster cross-flow, preferred for sources of increased fouling–scaling characteristics.

4. Theoretical model performance analysis of 7ME6 BWRO-CCD

The performance of BWRO-CCD units can be derived by theoretical model analysis at the level of an isolated sequence as well as for a continuous consecutive sequential process and this is illustrated in Table 3 for the NMEn (E = ESPA2-MAX; $N = 7$; $n = 6$) unit design displayed in Fig. 2 with seven modules each of six elements and feed of 2,000 ppm NaCl ($\pi = 1.60$) bar at 25°C which typifies common brackish water sources in the salinity range 2,300–2,500 ppm. It should be pointed out right from start that conventional computerized design programs of membranes manufacturers are unfit for complete BWRO-CCD simulations since this technology is based on different conceptual and operational principles compared with conventional techniques. In spite of aforementioned, isolated steps in the BWRO-CCD process could be ascertain with the aid of conventional design programs which provide valuable performance information pertinent to the specific membrane elements offered by their producers. The data base for the simulation at the top of Table 3 contains information regarding the specifications of the membrane elements; the design features of the unit (e.g. number elements and pressure vessels, volume of closed circuit,

Table 2
IMS design performance data for the ME4 (E = ESPA2-MAX) module with 2,500 ppm NaCl feed under the specified flow, flux, applied pressure and MR conditions at pH = 7.0 and 25°C without exceeding any of the computerized design program restrictions with regards to maximum beta (1.20) and flow conditions (e.g. 1.71 m^3/h maximum feed flow at inlet to module)

IMS design data: ESPA2-MAX; 2,500 ppm NaCl; pH = 7.0; Temperature = 25°C													Calculated terms from IMS design data					
	Flow				Flux			Pressure					Average		Recovery		*pf*-element	
Module design	Perm. m^3/h	Feed m^3/h	Conc. m^3/h	MR%	Averge lmh	Head lmh	Tail lmh	Head bar	Tail bar	Δp bar	*pf* beta factor	Perm. TDS ppm	Element Y_{av}	Module f_{av}	Head %	Tail %	Head factor	Tail factor
ME4	4.0	11.4	7.4	35.0	24.5	29.1	19.8	7.9	6.6	1.30	1.10	29.9	10.2	1.09	10.4	9.8	1.09	1.08
ME4	4.0	10.0	6.0	40.0	24.5	29.0	19.7	7.9	6.8	1.10	1.10	31.7	12.0	1.10	11.8	11.8	1.10	1.10
ME4	4.0	8.9	4.9	45.0	24.5	29.2	19.5	7.9	7.1	0.80	1.10	33.8	13.9	1.12	13.4	14.0	1.11	1.12
ME4	4.0	8.0	4.0	50.0	24.5	29.5	19.0	8.0	7.3	0.70	1.10	36.8	15.9	1.14	15.0	16.2	1.13	1.14
ME4	4.5	12.9	8.4	35.0	27.5	32.7	22.4	8.7	7.1	1.60	1.10	26.5	10.2	1.09	10.4	9.9	1.09	1.08
ME4	4.5	11.3	6.8	40.0	27.5	32.5	22.4	8.6	7.4	1.20	1.10	28.1	12.0	1.10	11.8	11.9	1.10	1.10
ME4	4.5	10.0	5.5	45.0	27.5	32.6	22.3	8.6	7.6	1.00	1.10	30.0	13.9	1.12	13.3	14.2	1.11	1.12
ME4	4.5	9.0	4.5	50.0	27.5	32.8	21.9	8.6	7.8	0.80	1.18	32.3	15.9	1.14	14.9	16.6	1.13	1.14
ME4	5.0	14.3	9.3	35.0	30.6	36.3	25.0	9.4	7.6	1.80	1.10	23.9	10.2	1.09	10.4	9.9	1.09	1.08
ME4	5.0	12.5	7.5	40.0	30.6	36.0	25.1	9.3	7.9	1.40	1.10	25.3	12.0	1.10	11.8	12.0	1.10	1.10
ME4	5.0	11.1	6.1	45.0	30.6	36.0	25.1	9.3	8.1	1.20	1.15	27.0	13.9	1.12	13.2	14.4	1.11	1.12
ME4	5.0	10.0	5.0	50.0	30.6	36.2	24.6	9.3	8.3	1.00	1.18	29.0	15.9	1.14	14.8	16.7	1.13	1.14
ME4	5.5	15.7	10.2	35.0	33.6	39.9	25.5	10.1	8.0	2.10	1.10	21.7	10.2	1.09	10.4	9.2	1.09	1.08
ME4	5.5	13.8	8.3	40.0	33.6	39.5	27.8	10.0	8.4	1.60	1.10	23.0	12.0	1.10	11.7	12.1	1.10	1.10
ME4	5.5	12.2	6.7	45.0	33.6	39.4	27.7	10.0	8.6	1.40	1.15	24.5	13.9	1.12	13.2	14.4	1.11	1.12
ME4	5.5	11.0	5.5	50.0	33.6	39.6	27.4	10.0	8.9	1.10	1.18	26.3	15.9	1.14	14.7	16.9	1.13	1.15
ME4	6.0	17.1	11.1	35.0	36.7	43.6	30.0	10.9	8.5	2.40	1.10	19.9	10.2	1.09	10.4	9.9	1.09	1.08
ME4	6.0	15.0	9.0	40.0	36.7	43.1	30.4	10.7	8.9	1.80	1.10	21.1	12.0	1.10	11.7	12.1	1.10	1.10
ME4	6.0	13.3	7.3	45.0	36.7	42.9	30.5	10.7	9.1	1.60	1.15	22.4	13.9	1.12	13.1	14.5	1.11	1.12
ME4	6.0	12.0	6.0	50.0	36.7	43.0	30.1	10.7	9.4	1.30	1.18	24.1	15.9	1.14	14.6	17.0	1.13	1.15

Table 3
Theoretical model sequence analysis for the BWRO-CCD NMEn (E = ESPA2-MAX; $N = 7$ and $n = 6$) unit with feed of 2,000 ppm NaCl under the fixed flow and pressure conditions of the PFD step [$Q_{HP} = 57.8\ m^3/h$; $Q_p = 11.6\ m^3/h$ and MR = 20%] and fixed flow and variable pressure conditions the CCD cycles [$Q_{HP} = Q_p = 42.8\ m^3/h$; $Q_{CP} = 23.1\ m^3/h$; MR = 65%] in a closed circuit volume of 769.8 L using pressure vessels (8´´) 630 cm long without any spacers at 25°C and assuming 75% efficiency of both pumps

Test Conditions		Unit Design		PFD		CCD		PUMPS	
40.8	m2/Element	7	Modules	0.200	% NaCl	0.25	% Initial feed	0.75	HP Efficiency.
45.4	m3/day	6	Elements/Module	35	% increased HP flow	25.0	lmh - Flux	0.75	CP Efficiency
1,500	ppm NaCl	630	cm, PV length	57.8	m3/h Feed	65	% Module Recovery		
10.5	bar Applied Pressure	20	cm, PV diameter	20	% Recovery	1.07	bar Δp		
15	% Recovery	2	%, added conduits	1.45	bar Δp	42.8	m3/h Permeate (=Q_{HP})		
25	°C	15	liter per element	11.6	m^3/h Permeate	23.1	m3/h Cross Flow (Q_{CP})		
99.6	% Salt Rejection	769.8	liter, Closed Circuit	46.3	m^3/h Brine	65.9	m3/h Module Inlet		
9.285	bar NDP			0.25	% Brine	1.43	m3/CCD-Cycle		
46.36	l/m2/h Flux	π - C Relationship		6.8	lmh - flux	2.00	min/cycle CCD		
4.416	l/m2/h/bar -A	1.6	bar , π Feed	1.00	min/step PFD	TEMPERATURE			
0.146	l/m2/h - B	8.00	π(bar)/C(%)	0.19	m3/step Permeate	25	°C		
				3.60	bar Applied Pressure	1.000	TCF		

General Information

3.7	% av-Element-PFD recovery
16.1	% av-Element-CCD recovery
1.03	av-pf - PFD
1.14	av-pf - CCD

ME6 Module Data				Separate CCD Cycles & PFD Step						Combined Sequence (CCD Cycles & PFD Step)						Permeate		
		Inlet	Outlet	Time	p_{appl}	HP	CP	HP+CP	per Step	Time	Permeate - m3		REC	Energy		mean	Step	mean
Mode	Step	%	%	min	bar	kW	kW	kW	kWh/m3	Σmin	Step	Σm3	%	ΣkWh	kWh/m3	m3/h	ppm	ppm
PFD	**0**	**0.20**	**0.25**	**1.0**	**3.6**	**7.7**	**0.00**	**7.71**	**0.666**	**1.0**	**0.192**	**0.19**	**20.0**	**0.128**	**0.666**	**11.6**	**50**	**50**
CCD	1	0.25	0.71	2.0	9.0	14.2	0.92	15.1	0.354	3.0	1.43	1.62	67.8	0.63	0.391	32.4	32	34
CCD	2	0.38	1.09	4.0	10.4	16.5	0.92	17.4	0.407	5.0	1.43	3.05	79.9	1.22	0.398	36.6	49	41
CCD	3	0.51	1.46	6.0	11.9	18.8	0.92	19.7	0.460	7.0	1.43	4.48	85.3	1.87	0.418	38.4	65	49
CCD	4	0.64	1.83	8.0	13.3	21.1	0.92	22.0	0.514	9.0	1.43	5.91	88.5	2.61	0.441	39.4	82	57
CCD	5	0.77	2.20	10.0	14.7	23.4	0.92	24.3	0.567	11.0	1.43	7.34	90.5	3.42	0.466	40.0	99	65
CCD	6	0.90	2.57	12.0	16.2	25.7	0.92	26.6	0.620	13.0	1.43	8.77	91.9	4.31	0.491	40.4	115	73
CCD	7	1.03	2.94	14.0	17.6	27.9	0.92	28.9	0.674	15.0	1.43	10.20	93.0	5.27	0.517	40.8	132	81
CCD	8	1.16	3.31	16.0	19.1	30.2	0.92	31.2	0.727	17.0	1.43	11.63	93.8	6.31	0.542	41.0	149	90
CCD	9	1.29	3.69	18.0	20.5	32.5	0.92	33.4	0.781	19.0	1.43	13.06	94.4	7.42	0.569	41.2	165	98
CCD	10	1.42	4.06	20.0	21.9	34.8	0.92	35.7	0.834	21.0	1.43	14.49	95.0	8.62	0.595	41.4	182	106
CCD	11	1.55	4.43	22.0	23.4	37.1	0.92	38.0	0.887	23.0	1.43	15.92	95.4	9.89	0.621	41.5	199	115
CCD	12	1.68	4.80	24.0	24.8	39.4	0.92	40.3	0.941	25.0	1.43	17.35	95.8	11.23	0.647	41.6	215	123
CCD	13	1.81	5.17	26.0	26.3	41.7	0.92	42.6	0.994	27.0	1.43	18.78	96.1	12.65	0.674	41.7	232	131
CCD	14	1.94	5.54	28.0	27.7	44.0	0.92	44.9	1.047	29.0	1.43	20.21	96.3	14.15	0.700	41.8	249	140
1	2	3	4	5	6	7	8	9	10	11	12	13	14	15	16	17	18	19

etc.) and flow conditions of the PFD step and CCD cycles of the two-step consecutive sequential process. The noteworthy features in Table 3 pertain to feed of 2,000 ppm NaCl at start of PFD performed with $Q_{HP} = 57.8\ m^3/h$, $Q_p = 11.6\ m^3/h$ and MR = 20% and feed of 2,500 ppm NaCl at start of CCD performed under fixed flow and variable pressure conditions with $Q_{HP} = Q_p = 42.8\ m^3/h$, $Q_{CP} = 23.1\ m^3/h$ and MR = 65% in a closed circuit volume of 769.8 L using pressure vessels (8´´) 630 cm long without any spacer(s) at 25°C and assuming 75% efficiency of both pumps. The simulation in the table describes the sequential progression of the CCD cycles under variable pressure and fixed flow conditions along a time scale with recovery achieved by the recycling of concentrate mixed with fresh feed at inlet to modules until the desired sequence recovery (henceforth "recovery") at a defined maximum applied pressure is attained. The set-point of the maximum applied pressure at the desired recovery level triggers the CCD → PFD shift, whereby brine is replaced by fresh feed and the resumption of CCD by the PFD → CCD shift is triggered when the flow meter volumetric signal of replaced brine matches the closed circuit volume of the design (769.8 L). The set-points for the CCD → PFD and PFD → CCD shifts enable the continuous desalination at the desired recovery by the non-stop consecutive sequential process under review.

The entire data in Table 3 is theoretically driven using conventional RO and power equations with

explanation provided below according to the labelled columns in the bottom of the table. The data base for the simulations is listed at the top of the table. The mode in the sequence is defined in column 1 and the step in column 2, wherein 0 stands for PFD and numbers for CCD cycles. The module inlet and outlet percentage concentrations are outlined in columns 3 and 4, respectively, and the period duration (minutes) of the PFD step and the cumulative CCD cycles are provided in column 5. The applied pressure (bar) during PFD and the variable applied pressures during CCD in column 6 are derived by Eq. (3), wherein, μ stands for flux, A for permeability coefficient, T_{CF} for temperature correction factor, $\Delta\pi_{av}$ for average concentrate-side osmotic pressure difference, Δp for module inlet–outlet pressure difference, p_p for permeate release pressure and π_p for average permeate-side osmotic pressure. The use of the mean osmotic pressure term $\Delta\pi_m$ as first approximation instead of $\Delta\pi_{av}$ generally leads to some higher pressure by ~10% and therefore, the latter term is important to generate more accurate applied pressure data. The term $\Delta\pi_{av}$ is derived from Eq. (4); wherein, C_f stands for feed concentration at inlet to modules and C_{av} for the average recycled concentrate cross-flow along the module and the substitution of C_{av} by the mean cross-flow value C_m provides a reasonable estimate of $\Delta\pi_{av}$. The term C_m/C_f in Eq. (4) is expressed by Eq. (5); wherein, C_f stands for the inlet feed concentration to modules and C_c for the recycled brine concentration from their outlets during CCD cycles. The term pf_{av} in Eq. (3) is derived from Eq. (2) and the term Δp from Eq. (6) for 8´´ pressure vessels wherein, n stands for the number of elements per module, q for the mean cross-flow (m^3/h) expressed by Eq. (7) and the exponent factor $z = 1.68 \pm 0.02$ which yields consistent results with IMS Design data for the ESPA2-MAX elements. The power (kW) for HP in column 7 is derived from Eq. (8) and for CP in column 8 from Eq. (9) and the sum of both pumps is listed in column 9.

$$p_{appl} = \mu/A/T_{CF} + \Delta\pi_{av} + \Delta p/2 + p_p - \pi_p \quad (3)$$

$$\Delta\pi_{av} = \pi_f * (C_{av}/C_f) * pf_{av} \approx \pi_f * (C_m/C_f) * pf_{av} \quad (4)$$

$$C_m/C_f = (C_f + C_c)/2/C_f = (1/2) * [1 + C_c/C_f] \quad (5)$$

$$\Delta p(\text{bar}) = (8/1,000) * n * q^z \quad (6)$$

$$q(\text{m}^3/\text{h}) = (Q_f + 2Q_{CP})/2 \quad (7)$$

$$P_{HP}(\text{kW}) = p_{appl} * Q_{HP}/36/f_{HP} \quad (8)$$

$$P_{CP}(\text{kW}) = \Delta p * Q_{CP}/36/f_{CP} \quad (9)$$

$$C_p = B * C_f * pf_{av} * T_{CF}/\mu \quad (10)$$

The specific energy (kWh/m^3) per PFD step or CCD cycle in column 10 is derived from the expression P (kW)/Q_p(m^3/h) for the PFD step and each of the CCD cycles. The combined (PFD + CCD) cumulative sequence period (minute) is provided in column 11. Permeates produced volumes (m^3) during the PFD step and CCD cycles are provided in column 12, their sequential accumulations (Σm^3) in column 13 which together with the fixed closed circuit intrinsic volume ($V = 769.8$ L) provide the sequential recovery data in column 14 expressed by $\Sigma V_p/(\Sigma V_p + V) \times 100$; wherein, ΣV_p stands for the cumulative sequential permeate volume and V for the intrinsic closed circuit volume. The process under review is essentially a consecutive sequential batch process and the aforementioned recovery expression is typical of such a batch desalination process. The cumulative energy (ΣkWh) of HP and CP during the sequential progression is provided in column 15 and this data combined with the relevant cumulative permeate volumes in column 13 (Σm^3) leads to the sequential mean specific energy terms in column 16 according to the expression $\Sigma kWh/\Sigma m^3$. Additional information in Table 3 pertinent to permeates includes the sequential mean permeate production flow rate (m^3/h) during the PFD-CCD progression in column 17, permeates TDS (ppm) per PFD step and CCD cycle in column 18 and their average value in column 19. Permeate TDS (ppm) is derived by Eq. (10) using the average concentration polarization factor (pf_{av}) derived by Eq. (2).

Since the CCD cycles are operated under fixed flow and variable pressure conditions, all parameters during the cycles remain unchanged and the differences between the cycles are manifested in the applied pressure and TDS of permeates. Comparison between the theoretical driven CCD parameters of the first cycle in Table 3 and the relevant IMS Design data (in parentheses) in line 6 of Table 1 for ME6 (E = ESPA2-MAX) are as follows: Fee 2,500 (2,500) ppm NaCl; MR = 65%(65%); flux = 25.0(24.5)lmh; $p_{appl} = 9.0$ (8.9) bar; $\Delta p = 1.07(1.00)$ bar; $pf_{av} = 1.14(1.15)$ factor; average element recovery = 16.1(16.1)% and permeate-TDS = 32.0(51.7) ppm. The only significant difference in the compared data under review relates to the TDS of permeates and since both results originate from the same salt diffusion expression Eq. (10),

wherein the principle parameters are either identical (B, C_f and T_{CF}) or very close to each other (pf_{av} and μ), the difference implies the use of a rejection factor under 99.6% by the IMS Design program or a value lower than that claimed by the manufacturer for such new elements. The aforementioned comparison validates the theoretical data in Table 3 for the entire sequence which comprises identical CCD cycles.

The translation of the sequential data in Table 3 into a continuous consecutive sequential process requires a set-point selection of maximum sequential applied pressure which triggers the CCO → PFD shift, whereby brine is replaced by fresh feed at the desired recovery. For example, the attainment of 90.5% recovery according to the data in Fig. 3 requires a maximum applied pressure set-point selection of 14.7 bar and this implies a sequence of five CCD cycles with an overall sequence period of 11.0 min of which 10.0 min involve CCD (91%) and 1.0 min PFD (9%) and such a process will produce an average permeate of 65 ppm TDS with an average flow rate of 40.0 m^3/h. The theoretical model sequence performance up to 92% recovery of the BWRO-CCD 7ME6 (E = ESPA2-MAX) unit design in Fig. 2 with feed of 2,000 NaCl ppm according to the data in Table 3 is displayed graphically as follows: Fig. 3(A–C) describes applied pressure variations as function of CCD cycles (A), sequence period (B) and recovery (C). Fig. 4(A–D) describes sequential power variations as function of CCD cycles (A) and recovery (B) as well as the respective variations of specific energy in (C) and (D). Fig. 5(A) and (B) describes sequential TDS variations of permeates as function of CCD cycles (A) and recovery (B).

5. Theoretical model analysis of 7MEn(n = 4–6) BWRO-CCD at different flux

The database in Table 3 for the 7ME6 unit with feed of 2,000 ppm NaCl may apply to the general class of BWRO-CCD NMEn (n = 4–6) units and such a comprehensive comparison for ~90% recovery is illustrated in Table 4 for the 7MEn(n = 4–6) series at the same flux (24.5 lmh) as function of MR (40–65%) and for the 7ME4 unit as function of flux (24.5; 27.5; 30.6; 33.6 and 36.7 lmh) and MR(40–50%). The same database for the PFD step in Table 3 (feed of 0.200% NaCl; 25% increased HP flow over CCD and MR = 20%) applies to all the simulated data in Table 4 and implies fixed flux of 6.1 lmh during PFD and brine of 0.25% at the start of CCD cycles.

5.1. Theoretical model analysis results for 7MEn(E = ESPA2-MAX; n = 4–6) BWRO-CCD Series under fixed flux conditions

According to Table 4, sequential operation of ~90.0% recovery (range: 89.8–90.5%) of said series of different module designs (ME6, ME5 and ME4) at the same flux (24.5 lmh) with increased MR leads to higher average element recovery (av-Elem) and average concentration polarization factor (pf_{av}); smaller number of CCD cycles, lower CCD pressure at start

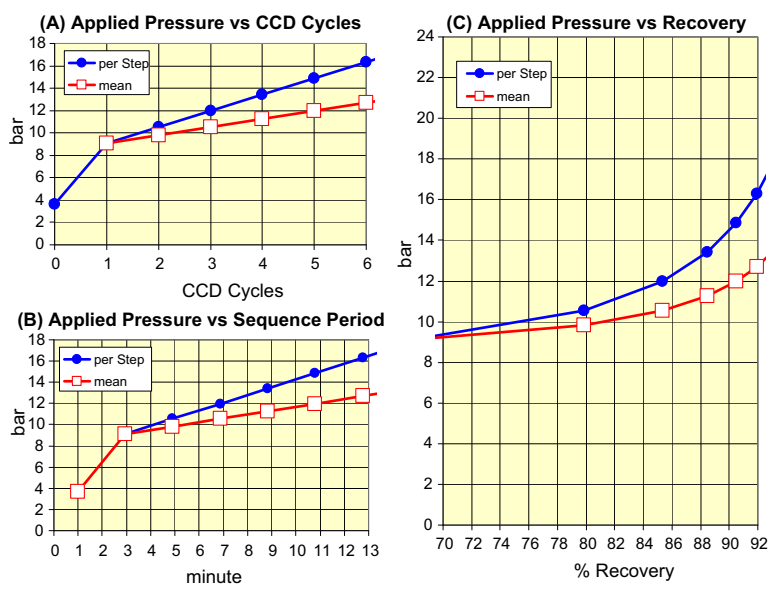

Fig. 3. Sequential applied pressure variations as function of CCD cycles (A), sequence period (B) and recovery (C) according to the data furnished in Table 3.

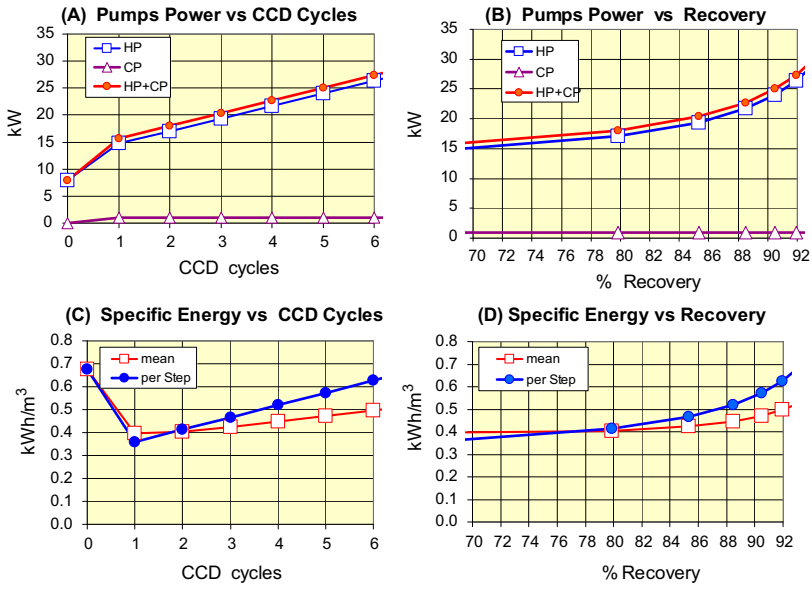

Fig. 4. Sequential power variations as function of CCD cycles (A) and recovery (B) and the respective specific energy variations as function of CCD cycles (C) and recovery (D) according to the data furnished in Table 3.

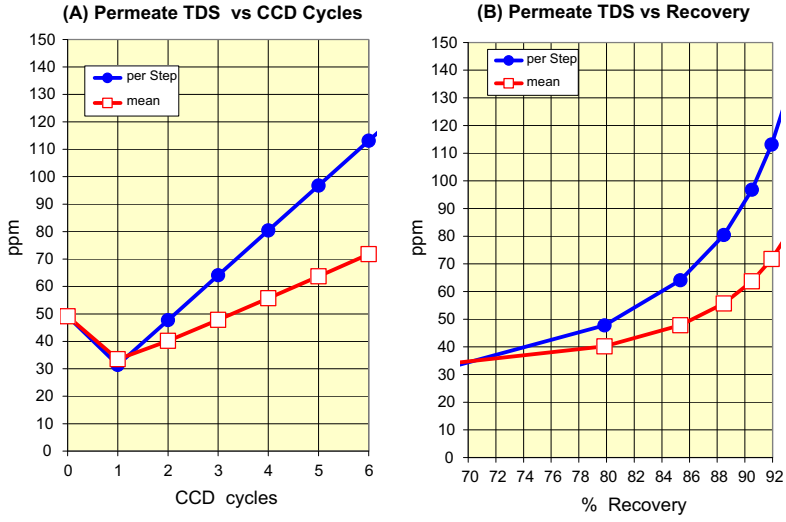

Fig. 5. Sequential TDS variations of permeates as function of CCD cycles (A) and recovery (B) according to the data furnished in Table 3.

and end of each sequence, smaller pressure difference in modules (Δp), lower specific energy and minor variations in TDS of permeates and their production rates per design. A deceased number of elements per module (ME6 > ME5 > ME4) in the designs under review at the same flux (e.g. 24.5 lmh), MR (e.g. MR=45%) and recovery (e.g. ~90%) reveal increased average element recovery (e.g. av-Elem: 9.6 < 11.3 < 13.9%) and the average concentration polarization factor (e.g. pf_{av}: 1.08 < 1.10 < 1.20); decreased CCD pressure at start (e.g. 8.7 > 8.3 > 8.1 bar) and end (e.g. 16.2 > 15.9 > 15.8 bar) of CCD cycles as well as decreased pressure difference (e.g. Δp: 2.3 > 1.4 > 0.8 bar), specific energy (e.g. 0.565 > 0.513 > 0.481 kWh/m^3) and rates of permeates production (e.g. 38.8 > 32.4 > 25.9m^3/h) with minor changes, if any, associated with of the number of CCD cycles per sequence (e.g. 11→11→11 CCD cycles), permeates TDS (e.g. 63→64→65 ppm) and sequence periods (e.g. 11.0→11.2→11.5 min).

Table 4
Comparative theoretical model analysis results for ~90% recovery of the BWRO-CCD 7MEn (E = ESPA2- MAX; n = 4–6) series according to the data base in Fig. 3 with the specified alterations of design features, flux and MR for feed of 2,000 ppm NaCl at 25°C assuming 75% efficiency of both pumps (HP and CP)

Design				CCD cycles performance					Consecutive sequential process									
PV	MOD	Elements							CCD	SEQ	CCD PRES (bar)			SEQ	SEQ	Perm.	Production	
cm	no.	MOD	Total	MR %	Feed %	Flux lmh	av-Elem %	pf_{av} factor	cycles	REC	Start	End	Δp	min	kWh/m^3	ppm	m^3/h	m^3/d
630	7	6	42	40	0.25	24.5	8.2	1.07	13	89.9	9.0	16.5	2.9	10.6	0.632	62	38.7	929
630	7	6	42	45	0.25	24.5	9.5	1.08	11	90.2	8.7	16.2	2.3	11.0	0.565	63	38.8	932
630	7	6	42	50	0.25	24.5	10.9	1.09	9	90.2	8.6	15.6	1.8	11.0	0.519	63	38.8	932
630	7	6	42	55	0.25	24.5	12.5	1.11	7	89.8	8.6	14.8	1.5	10.5	0.482	61	38.7	929
630	7	6	42	60	0.25	24.5	14.2	1.12	6	90.2	8.7	14.7	1.2	11.0	0.467	64	38.8	932
630	7	6	42	65	0.25	24.5	16.1	1.14	5	90.5	8.8	14.6	1.0	11.3	0.457	66	38.9	934
530	7	5	35	40	0.25	24.5	9.7	1.08	13	89.9	8.4	16.1	1.8	10.8	0.553	62	32.3	775
530	7	5	35	45	0.25	24.5	11.3	1.10	11	90.2	8.3	15.9	1.4	11.2	0.513	64	32.4	777
530	7	5	35	50	0.25	24.5	12.9	1.11	9	90.2	8.3	15.4	1.1	11.2	0.484	64	32.4	777
530	7	5	35	55	0.25	24.5	14.8	1.13	7	89.8	8.4	14.7	0.9	10.7	0.458	63	32.2	774
530	7	5	35	60	0.25	24.5	16.7	1.15	6	90.2	8.5	14.7	0.7	11.2	0.451	65	32.4	777
430	7	4	28	40	0.25	24.5	12.0	1.10	13	89.9	8.1	15.9	1.1	11.1	0.507	64	25.8	620
430	7	4	28	45	0.25	24.5	13.9	1.12	11	90.2	8.1	15.8	0.8	11.5	0.481	65	25.9	621
430	7	4	28	50	0.25	24.5	15.9	1.14	9	90.2	8.2	15.4	0.6	11.5	0.463	66	25.9	621
530	7	4	28	40	0.25	27.5	12.0	1.10	13	89.9	8.9	16.7	1.3	14.0	0.545	57	29.0	695
530	7	4	28	45	0.25	27.5	13.9	1.12	11	90.2	8.9	16.6	1.0	14.5	0.518	58	29.1	697
530	7	4	28	50	0.25	27.5	15.9	1.14	9	90.2	8.9	16.2	0.8	14.5	0.496	59	29.1	697
530	7	4	28	40	0.25	30.6	12.0	1.10	13	89.9	9.7	17.5	1.5	12.6	0.590	51	32.2	774
530	7	4	28	45	0.25	30.6	13.9	1.12	11	90.2	9.7	17.4	1.2	13.0	0.556	52	32.3	776
530	7	4	28	50	0.25	30.6	15.9	1.14	9	90.2	9.7	17.0	0.9	13.0	0.531	53	32.3	776
530	7	4	28	40	0.25	33.6	12.0	1.10	13	89.9	10.5	18.3	1.8	11.5	0.634	46	35.4	850
530	7	4	28	45	0.25	33.6	13.9	1.12	11	90.2	10.4	18.1	1.4	11.9	0.595	48	35.5	852
530	7	4	28	50	0.25	33.6	15.9	1.14	9	90.2	10.4	17.7	1.1	11.9	0.566	48	35.5	852
530	7	4	28	40	0.25	36.7	12.0	1.10	13	89.9	11.4	19.1	2.1	10.5	0.681	42	38.7	928
530	7	4	28	45	0.25	36.7	13.9	1.12	11	90.2	11.3	19.0	1.6	10.9	0.635	44	38.8	931
530	7	4	28	50	0.25	36.7	15.9	1.14	9	90.2	11.2	18.5	1.3	10.9	0.602	44	38.8	931

Performance comparison between the 7ME6, 7ME5 and 7ME4 units of the different module designs at ~90.0% recovery under fixed flux (24.5 lmh) and variable pressure conditions as function of MR are illustrated for the initial and final CCD applied pressures of 7ME6 in Fig. 6(A), 7ME5 in Fig. 6(B) and 7ME4 in Fig. 6(C). Variations as function module design and MR are displayed in Fig. 7(A) for average element recovery; in Fig. 7(B) for concentration polarization; in Fig. 7(C) for modules' pressure difference; in Fig. 8(A) for specific energy; in Fig. 8(B) for permeate TDS and in Fig. 8(C) of sequence periods. The results in Table 4 and Figs. 6–8 are generated from theory and therefore, are fully consistent with the fundamental principles of RO. Moreover, the results in Table 4 are also consistent with the IMS Design data for such modules with ESPA2-MAX elements, leaving no doubt concerning the reliability of the compared data and its practical ramifications. MR variations in the context of CCD imply cross-flow variations, since $MR = Q_p/(Q_f + Q_{CP}) \times 100 = Q_f/(Q_f + Q_{CP}) \times 100$, with increased MR associated with decreased cross-flow (Q_{CP}) and vice versa. Desired cross-flow and flux in CCD are set-point selections independent of each other and therefore of immediate practical significance in the operation of this noteworthy technology.

5.2. Theoretical model analysis results for 7MEn(E = ESPA2-MAX; n = 4–6) BWRO-CCD series under variable flux conditions

The flux variations effects in Table 4 are ascertained in the context of the 7ME4 unit design, since according to the IMS Design data in Table 1 this noteworthy module operates with a rather narrow flux distribution range of high uniformity and thereby, enables the attainment of high flux operation with maximum (head element) and minimum (tail element) not fare removed from the average flux and well within the recommended parameters (e.g. head element recovery, concentration polarization, permeate-brine flow ratio, feed flow at inlet to modules, etc.) by membrane elements producers. The first unit design of 7ME4 configuration in Table 4 that for 24.5 lmh flux contains pressure vessels 430 cm long; whereas, the second unit design configuration for the flux range 27.5–36.7 lmh contains 530 cm long pressure vessels with spacers equivalent in length to a single element, and this structural difference has no effect on the performance characteristics of the system except for sequence period duration–the design with longer pressure vessels is intended to assure sequence periods greater than 10 min when flux raised above 24.5 lmh.

The flux performance effects on the BWRO-CCD 7ME4 unit at ~90% recovery with 2,500 ppm NaCl CCD feed and MR of 40, 45 and 50% are best illustrated graphically in relations to the various process parameters, a subject matter considered next. The final and initial CCD applied pressures in the system under review displayed in Fig. 9(A) and (B), respectively, reveal small variability with respect to flux and MR%. The applied pressure according to Eq. (3) is determined primarily by flux and to a much lesser degree by Δp and $\Delta\pi_{av}$ and since the initial feed (0.25%) and final brine (2.0%) concentrations in the system under

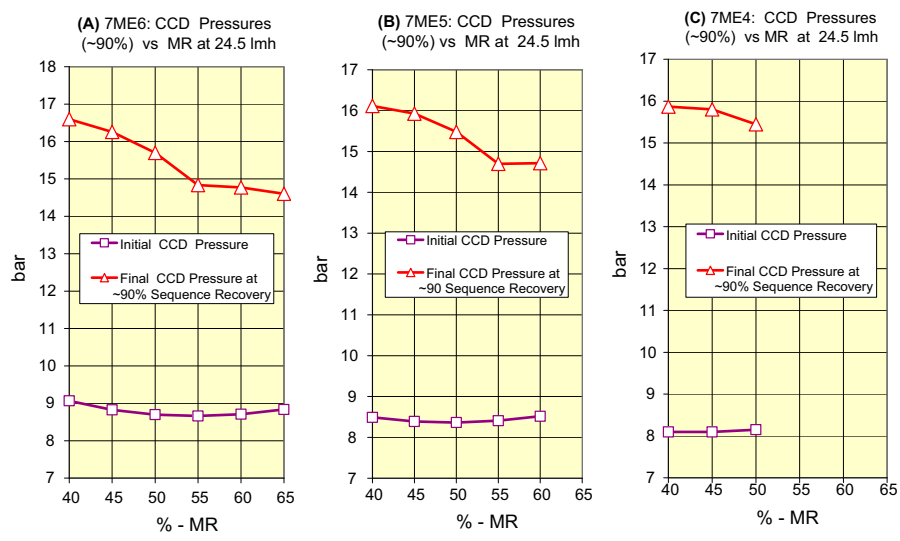

Fig. 6. Applied pressure requirements for ~90% recovery of 2,500 ppm NaCl CCD feed at 25˚C with fixed flux (24.5 lmh) as function of MR (40–65%) for the 7ME6 (A), 7ME5 (B) and 7ME4 (C) designed BWROP-CCD units according to the data in Table 4.

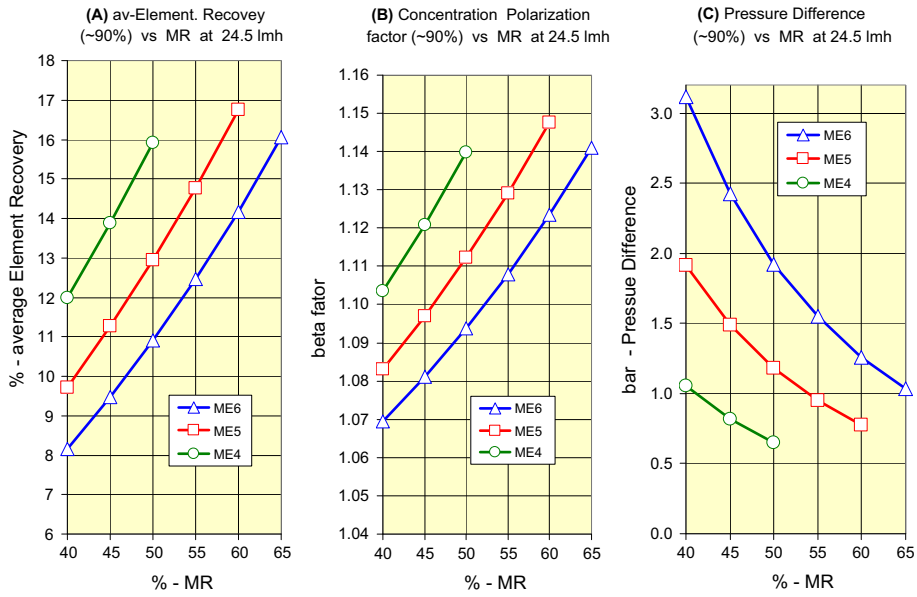

Fig. 7. Variations of average element recovery (A), concentration polarization—beta factor (B), and module pressure difference (C) for ~90% recovery of 2,500 ppm NaCl CCD feed at 25˚C with fixed flux (24.5 lmh) as function of MR (40%–65%) and module design (ME6, ME6 and ME4) according to the data in Table 4.

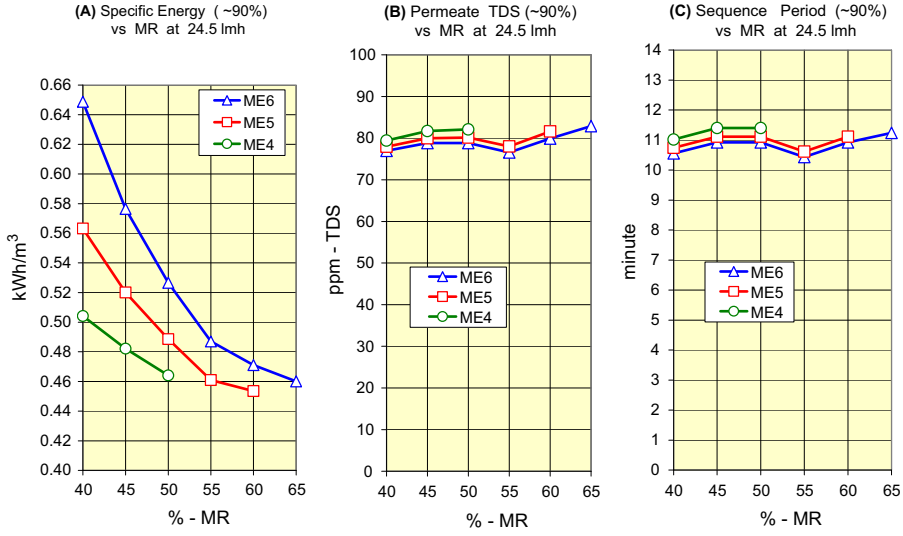

Fig. 8. Variations of specific energy (A), permeates TDS (B), and sequence periods (C) for ~90% recovery of 2,500 ppm NaCl CCD feed at 25˚C with fixed flux (24.5 lmh) as function of MR (40–65%) and module design (ME6, ME6 and ME4) according to the data in Table 4.

review remain unchanged irrespective flux, the small observed pressure differences most probably reflect Δp variations known to be influenced by flux and MR%.

Sequence period variations of 7ME4 at ~90% recovery in the system under consideration displayed in Fig. 9(C) as function flux (μ) and MR are fully understood from theory in light of the intrinsic closed circuit intrinsic (V) in the designs. The sequence period (T) expressed by Eq. (11) in is the sum of the PFD time (T_{PFD}) expressed in minute by Eq. (12) and the CCD time (T_{CCD}) expressed in minute by Eq. (13); wherein, V stands for the intrinsic closed circuit volume (litre) of the unit, Q_b(m^3/h) for brine flow rate during PFD, Q_f and Q_p (m^3/h) for feed and permeate flow rates

during CCD, R for sequence recovery (%), N for number of module per design, n for the number of elements per module, S (m^2) for membrane surface area per element and μ (lmh) for flux. In BWRO-CCD processes of the type considered hereinabove T_{PFD} (10–15% of T) according to Eq. (12) will remain unchanged under fixed PFD conditions; whereas, T_{CCD} according to Eq. (13) depends on sequence recovery (R), intrinsic volume (V) and CCD flux (μ) independent of MR. Accordingly, sequence duration of the 7ME4 design with fixed R and V terms should relate to flux and independent of MR. The variations of sequence periods with flux in Fig. 9(C) are self evident with increase μ leading to shorter T and vice versa. The intrinsic volume (V) effect on T is manifested in Fig. 9(C) by the much lower T value for the 7ME4 design with 430 cm long pressure vessels at 24.5 lmh compared with the related design with 530 cm long pressure vessels at 27.5 lmh.

$$T = T_{PFD} + T_{CCD} \tag{11}$$

$$T_{PFD} = V/Q_b * 1000/60 \tag{12}$$

$$\begin{aligned} T_{CCD} &= R * V/[Q_f * (100 - R)] \\ &= R * V/[Q_p * (100 - R)] \\ &= R * V/[(\mu * N * n * S/1000) * (100 - R)] \end{aligned} \tag{13}$$

The CCD average element recovery according Eq. (1) and the concentration polarization factor according to Eq. (2) in the 7ME4 deign under review are only a function of MR and therefore, independent of flux and/or sequence recovery and these features are evident in Fig. 10(A) and (B), respectively. In contrast, the pressure difference term (Δp) according to Eq. (6) and Eq. (7) is a function of flow rates at inlet and outlet of modules and therefore, depends on the permeation flux and flow rate of recycled concentrate (Q_{CP}) which define MR according to Eq. (14) and this explains the finding displayed in Fig. 10(C). Increased flux and MR also imply increased cross-flow (Q_{CP}) and average cross-flow and therefore, increased Δp in a defined design of unchanged N, S and n terms as in the case of the 7ME4 unit design under review.

The daily production rates of the 7ME4 design as function of flux (24.5 → 36.7 lmh) displayed in Fig. 11(A) are independent of MR and this implies the flexible selection of cross-flow irrespective of flux, a feature not possible by any other BWRO technique. The TDS of permeates as function of flux and MR displayed in Fig. 11(B) illustrates a sharp decrease of TDS with increased flux as well as a secondary effect of lower TDS with lower MR as results of declined concentration polarization and these observations are in accordance of the salt rejection expression in Eq. (10). Most (~97%) of the specific energy displayed in Fig. 11(C) as function of flux and MR originates for

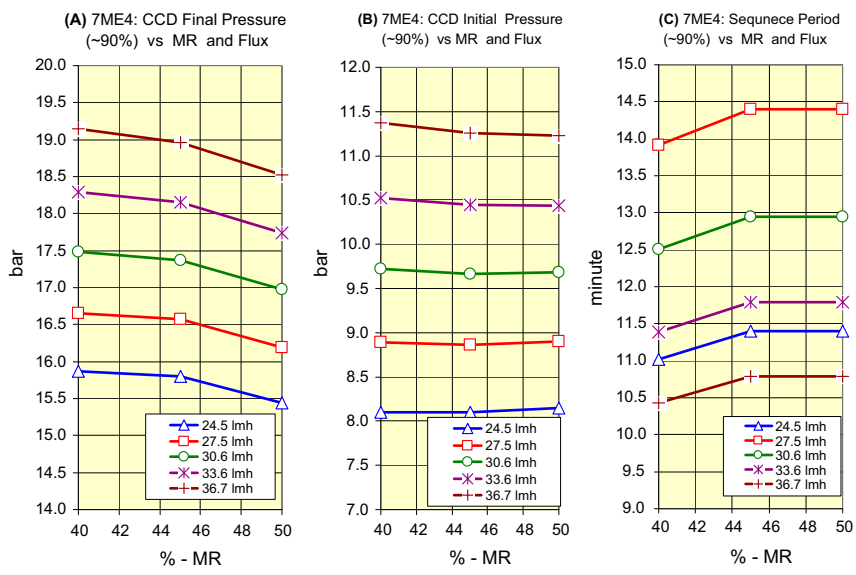

Fig. 9. Variations of CCD final pressure (A) and initial pressure (B) and sequence period (C) during ~90% recovery of 2,500 ppm NaCl CCD feed at 25°C as function of flux (24.5–36.7 lmh) and MR (40–45%) of the BWRO-CCD 7ME4 (E = ESPA2-MAX) unit according to the data in Table 4.

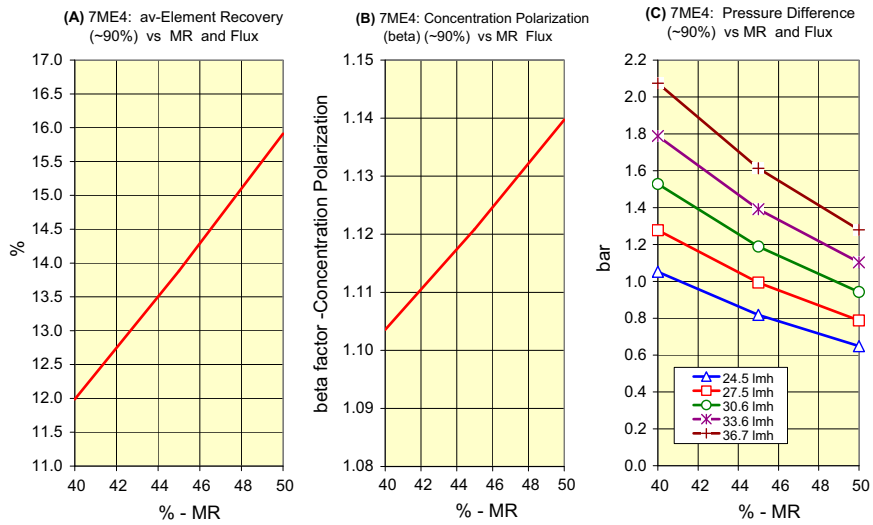

Fig. 10. Variations of CCD average element recovery (A), concentration polarization factor (B) and pressure difference (C) during the ~90% recovery of 2,500 ppm NaCl CCD feed at 25˚C as function of flux (24.5–36.7 lmh) and MR (40–45%) of the BWRO-CCD 7ME4 (E = ESPA2-MAX) unit according to the data in Table 4.

the CCD cycles of the sequence and includes the SE_{CP} (Eq. (15)), SE_{HP} (Eq. (16)) components and their total SE_{total} (Eq. (17)) and a minor part of the total energy originates from the PFD step of the process. The SE_{HP} during CCD is independent of the permeate flow rate which is the same as the pressurized feed flow rate and the term p_{av} in Eq. (16) stands for the CCD average variable applied pressure in the process and its dependence on flux is evident from Eq. (3). The SE_{CP} contribution to SE_{total} depends on the cross-flow created by the CP with increased MR associated with decreased cross-flow resulting in a lower contribution and vice versa. For example, the average relative SE_{CP} contribution to SE_{total} in the 7ME4 design under review at ~90% recovery with MR = 50% is 5.18% at 24.5 lmh and 7.86% at 36.7 lmh; whereas, with MR = 40% the respective values are 12.73 and 18.08% due to the increased cross-flow in the latter case.

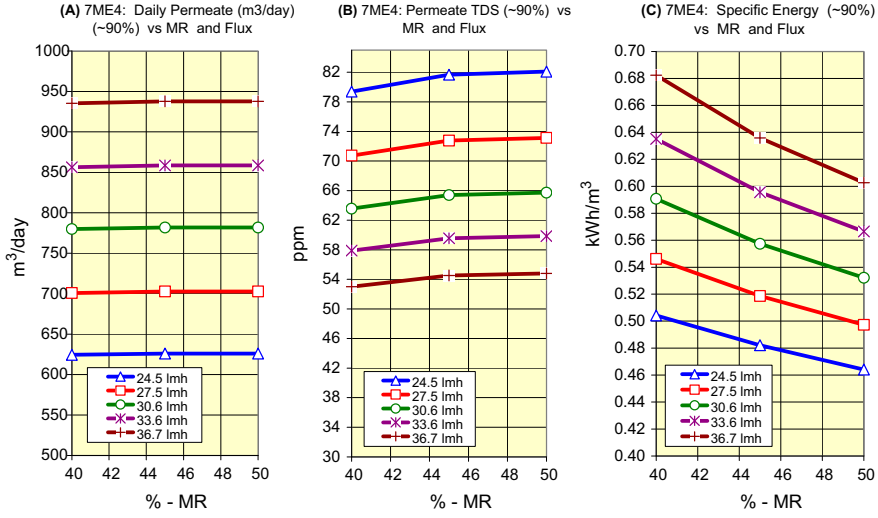

Fig. 11. Variations of the daily permeate production (A), permeate TDS (B), and specific energy (C) during the ~90% recovery of 2,500 ppm NaCl CCD feed at 25˚C as function of flux (24.5–36.7 lmh) and MR (40–45%) of the BWRO-CCD 7ME4 (E = ESPA2-MAX) unit according to the data in Table 4.

$$\mathrm{MR} = Q_f/(Q_f + Q_{\mathrm{CP}}) * 100 = (1/10) * (\mu * n * N * S) / (\mu * n * N * S/1000 + Q_{\mathrm{CP}}) \quad (14)$$

$$\mathrm{SE}_{\mathrm{CP}} = Q_{\mathrm{CP}} * \Delta p/36/f_{\mathrm{CP}}/Q_p = (1000/36) * (Q_{\mathrm{CP}} * \Delta p/f_{\mathrm{CP}})/(\mu * n * N * S) \quad (15)$$

$$\mathrm{SE}_{\mathrm{HP}} = p_{\mathrm{av}}/36/f_{\mathrm{HP}} \quad (16)$$

$$\mathrm{SE}_{\mathrm{total}} = p_{\mathrm{av}}/36/f_{\mathrm{HP}} + Q_{\mathrm{CP}} * \Delta p/36/f_{\mathrm{CP}}/Q_p = (1/36) * [p_{\mathrm{av}}/f_{\mathrm{HP}} + (1000 * Q_{\mathrm{CP}} * \Delta p/f_{\mathrm{CP}}) / (\mu * n * N * S)] \quad (17)$$

5.3. Theoretical assessment of modules with 4–6 elements for BWRO-CCD applications

The CCD technology operates with low energy and any desired high recovery irrespective of the number of elements per modules, confined only by the feed composition, the extensiveness of the pre-treatment and the membranes producers' recommendations of safe performance conditions some of which are revealed by the test conditions of elements. The aforementioned was demonstrated [10–14] for seawater desalination with the SWRO-CCD NMEn (M = SWC6; $N = 4$ and $n = 1$–4) units which revealed near theoretical energy consumption with 50% recovery without need for energy recovery means as well as for various BWRO-CCD NMEn ($n = 3$–4) applications [15–19]. The current theoretical study provides a comprehensive comparison between the various high recovery (~90%) performance aspects of modules with 4, 5 and 6 elements each in the context of the 7MEn ($n = 4$–6) designs under different flux (24.5–36.7 lmh) and MR (40–65%) conditions. The performance of the MEn ($n = 4$–6) modules are assessed by means of theoretical model simulations of complete sequences (PFD-CCD) as well as with IMS Design data of isolated steps in the process in order to confirm the theoretical results. The focus on modules with 4–6 elements is not a coincidence, since units with such

Table 5
Theoretical model data base for a 3-stage 4ME6-2ME6-ME6 conventional BWRO system of the design displayed in Fig. 1 with ESPA2-MAX elements; wherein, all the parameters are calculated by the same equations used in Table 3 for BWRO-CCD with feed of 2,000 ppm NaCl at 25°C and assuming 75% efficiency of HP and the inter-stage Booster Pumps (BP-1) and PB-2)

MEMBRANE	STAGE-1	STAGE-2	STAGE-3	SUMAMRY
TEST CONDITIONS	4 modules	2 modules	1 modules	7 Modules
ESPA2-MAX	6 elements/module	6 elements/module	6 elements/module	42 elements
40.8 m2/Element	24 total elements	12 total elements	6 total elements	
45.4 m3/day				
1,500 ppm NaCl	50 % Recovery	50 % Recovery	50 % Recovery	87.5 % RECOVERY
10.5 bar Applied Pressure	0.200 % inlet concen.	0.400 % inlet concen.	0.800 % inlet concen.	0.200 % inlet
15 % Recovery	0.400 % outlet concen.	0.800 % outlet concen.	1.600 % outlet concen.	1.600 % outlet
25 °C	46.3 m3/h feed	23.2 m3/h feed	11.6 m3/h feed	46.3 m3/h feed
99.5 % Salt Rejection	23.2 m3/h outlet brine	11.6 m3/h outlet brine	5.8 m3/h outlet brine	5.8 m3/h Brine
9.285 bar NDP	**23.2 m3/h permeate**	**11.6 m3/h permeate**	**5.8 m3/h permeate**	40.5 m3/h Permeate
46.36 l/m2/h Flux	23.6 lmh Flux	23.6 lmh Flux	23.6 lmh Flux	23.6 lmh average
4.416 l/m2/h/bar -A	1.60 bar π-inlet	3.20 bar π-inlet	6.40 bar π-inlet	
0.182 l/m2/h - B	3.20 bar π-outlet	6.40 bar π-outlet	12.80 bar π-outlet	
	0.11 ratio Y_{av}-(av-Elem.)	0.11 ratio Y_{av}-(av-Elem.)	0.11 ratio Y_{av}-(av-Elem.)	
	1.10 pf_{av}	1.10 pf_{av}	1.10 pf_{av}	
0.20 % NaCl Feed	2.64 $\Delta\pi_{av}$	5.27 $\Delta\pi_{av}$	10.55 $\Delta\pi_{av}$	
1.60 bar, osmotic pressure	1.81 bar Δp	1.81 bar Δp	1.81 bar Δp	
8.00 π(bar)/C(%) - assumed	8.90 bar applied	11.53 bar applied	16.81 bar applied	
	7.09 bar brine	4.45 bar -Booster	11.53 bar -Booster	
	0.75 efficiency ratio HP	0.75 efficiency ratio BP-1	0.75 efficiency ratio BP-2	
25 C° Temperature	15.26 kW power	3.81 kW power	7.21 kW power	26.28 kW
1.000 TCF	0.659 kWh/m3	0.330 kWh/m3	1.245 kWh/m3	0.649 kWh/m3
TCF=EXP[3020(1/298-1/(273+C)]	**25.4 ppm Permeate**	**50.8 ppm Permeate**	**101.5 ppm Permeate**	43.5 ppm Permeate

Table 6
Performance comparison between a conventional BWRO system (4ME6-2ME6-ME6) and a 7ME6 BWRO-CCD unit of the same number and type of elements (E = ESPA2-MAX) with the same feed source (2,000 ppm NaCl) at 25°C under similar recovery and flux conditions

4ME6+2ME6+ME6 (ESPA2-MAX) conventional BWRO design													7ME6 (ESPA2-MAX) CCD–MR = 65% PFD-MR = 20%							
Feed		Recovery			Inlet pressure			Final average production data								Final permeate production				
																	Average data			
TDS %	Inlet m³/h	R1 %	R2 %	R3 %	S1 bar	S2 bar	S3 bar	Flux lmh	Flow m³/h	TDS ppm	REC %	Energy kWh/m³	CCD MR %	PFD MR%	CCD cycles no.	REC %	m³/h	lmh	ppm	kWh/m³
0.20	43.7	40	40	40	7.2	9.9	13.9	20.0	34.3	37.6	78.4	0.706	65	20	2	79.9	37.3	21.8	50	0.404
0.20	43.7	45	45	45	7.9	10.5	14.8	21.3	36.4	40.9	83.4	0.654	65	20	3	85.3	39.2	22.8	60	0.424
0.20	43.7	50	50	50	8.5	11.1	16.4	22.3	38.2	46.1	87.5	0.625	65	20	4	88.5	40.2	23.4	70	0.447
0.20	43.7	55	50	50	9.2	11.1	17.0	22.6	38.8	50.2	88.8	0.608	65	20	5	90.5	40.8	23.8	80	0.471
0.20	43.7	60	55	50	10.0	12.2	18.8	23.2	39.8	58.4	91.0	0.602	65	20	6	91.9	41.2	24.1	90	0.497
0.20	43.7	65	55	50	10.8	12.5	20.3	23.5	40.3	65.5	92.1	0.606	65	20	7	93.0	41.6	24.3	100	0.522
0.20	43.7	65	60	50	10.8	13.7	22.0	23.7	40.6	70.0	93.0	0.612	65	20	8	93.8	41.8	24.4	110	0.548
0.20	43.7	65	65	50	10.8	15.1	24.3	23.9	41.0	76.0	93.9	0.622	65	20	9	94.4	42.0	24.5	120	0.574
0.20	43.7	65	65	55	10.8	15.1	26.4	24.1	41.3	78.1	94.5	0.628	65	20	10	95.0	42.2	24.6	130	0.600
0.20	43.7	65	65	60	10.8	15.1	29.0	24.3	41.6	80.8	95.1	0.637	65	20	11	95.4	42.3	24.7	140	0.627
0.20	43.7	65	65	65	10.8	15.1	32.4	24.4	41.8	84.4	95.7	0.648	65	20	12	95.8	42.4	24.8	151	0.653
								23.0										23.9		

configurations should be particularly suitable for large-scale BWRO-CCD applications.

All three module configurations ME4 (MR = 40–50%), ME5 (MR = 40–60%) and ME6 (40–65%) show viable high recovery and low energy BWRO-CCD performance characteristics in the indicated (brackets) MR ranges at an ordinary operational flux (24.5 lmh) without exceeding any of the limits specified for the ESPA2-MAX element in its test conditions. If high recovery (>88%) dictated by the feed source compositions and quality is attainable, pressure vessels of such modules do not require spacers since sequence periods exceed the desired minimum of 10-11 min and in this context one spacer per pressure vessel will be required for the recovery range 85–88% and two spacers for the recovery range 80–85%.

The comparative study results considered hereinabove appear to suggest the preference of the ME4 module configuration over ME5 and ME6 for reasons of greater versatility and flexibility in light of its lowest flux spread between head to tail elements and lowest module pressure difference under the same average operational flux and MR conditions with only a marginal increase in concentration polarization factor and the aforementioned implies an extraordinarily wide operational range of flux within the recommended membrane performance specifications by their manufacturers. In simple terms, the 7ME4 unit according to the data in Table 4 could be operated in the flux range 24.5–36.7 lmh, produce 620–931 m^3/d of permeates in the TDS range 64–42 ppm for source equivalent to 2,500 ppm NaCl CCD feed with energy of 0.507–0.681 kWh/m^3 depending on the MR (40–50%) with the lower energy range associated with MR = 50% and the above cited prospects with a relatively small flux spread between head and tail elements and low fouling characteristics for reasons discussed elsewhere. Incidentally, even at an extremely high average operational flux of 36.7 lmh the maximum head element flux of the ME4 (E = ESPA2-MAX) module reach 43.6 lmh, a value significantly lower than that under the test conditions of 46.35 lmh advised by the producer of said element.

The preference of ME4 over ME5 and ME6 module configurations with respect to reduced fouling characteristics originates from the following reasons: The number of CCD cycles required to reach a desired recovery is only a function of MR irrespective of number of elements per module; however, reaching of the desired recovery with the shorter ME4 module proceed with a smaller flux gap of greater performance uniformity of elements under lesser constrain on the head and tail elements which are more prone to fouling factors. Moreover, the cross-flow in ME4 could be

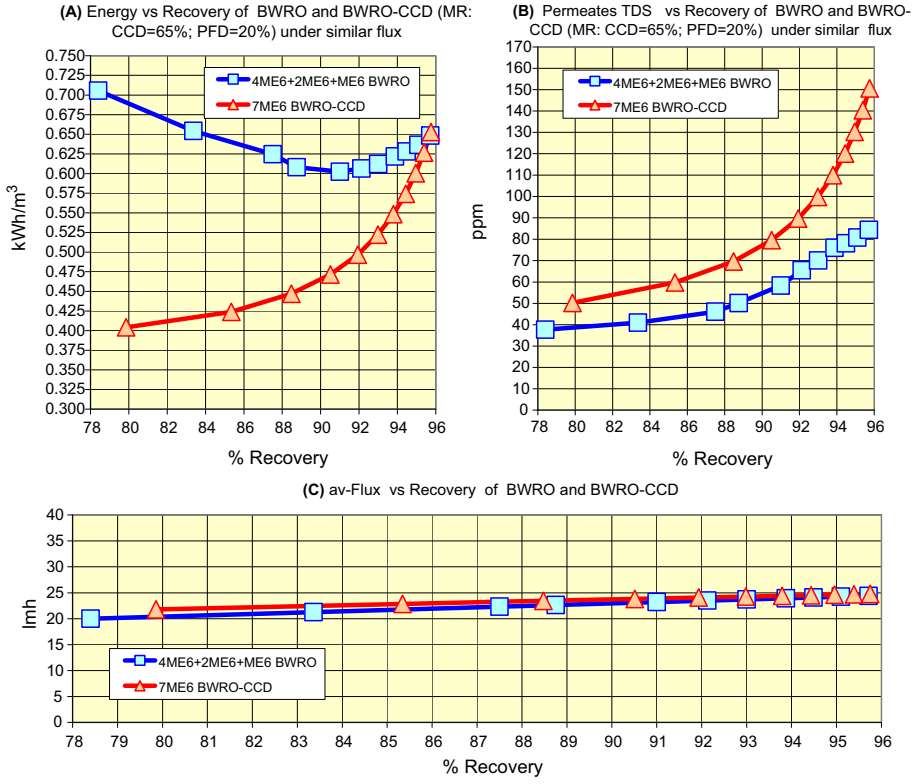

Fig. 12. Energy consumption (A), TDS of permeates (B) and average flux (C) as function of recovery for conventional BWRO and BWRO-CCD according to the data in Table 6.

increased by MR decrease under 40% without change of flux and this will result with a further increase in the number of CCD cycles required to reach a desired recovery and effect further reduction in the average recovery of the head and tail elements as well as their respective concentration polarization factors; thereby, assist in the optimization of the system towards reduced fouling due to particulate matter and/or scaling and/or biological factors.

6. Theoretical model performance comparison between the BWRO-CCD 7ME6 design and a conventional 3-stage 4ME6-2ME6-ME6 system

Reliable and effective comparison between the conventional and BWRO-CCD technologies requires focusing on the same feed system, designs of the same number of modules and elements with the same membrane elements and addressing the same pertinent issues of recovery, flux, energy and salt rejection using calculations performed with the same principle equations. The pertinent theoretical data base of the conventional approach which meets the above cited criteria is displayed in Table 5 and illustrates a conventional 3-stage 4ME6-2ME6-ME6 BWRO system with ESPA2-MAX elements; wherein, all the parameters are calculated by the same equations used in the context of Table 3 for the 7ME6 BWRO-CCD unit with feed of 2,000 ppm NaCl at 25˚C and assuming 75% efficiency of HP and the inter-stage booster pumps (BP-1) and PB-2). The comparison requires the presence of modules with six elements per vessel since this is the only way to enable recovery over 85% by means of the conventional BWRO approach. The data displayed in Table 5 shows an overall recovery of 87.5% reached by assuming 50% recovery per stage of ME6 modules and increase system recovery is concomitant with increased recovery per stage within the restrictions of the concentration polarization factors as determined by the average element recovery per each of the stages in the process. Increased system recovery in the model system under review is achieved by the systematic increase of recovery in the first stage (50–65%), then in the second stage and finally in the third stage of the process. The summary section in Table 5 takes account of the total permeates production and power requirements during the stages and this data applies to calculate the overall specific energy term of

Table 7
Performance comparison between a conventional BWRO system (4ME6-2ME6-ME6) and a 7ME6 BWRO-CCD unit with PFD-MR = 0% of the same number and type of elements (E = ESPA2-MAX) with the same feed source (2,000 ppm NaCl) at 25°C under similar recovery and flux conditions

4ME6+2ME6+ME6 (ESPA2-MAX) conventional BWRO design													7ME6 (ESPA2-MAX) CCD–MR = 65% PFD-MR = 0%								
Feed		Recovery			Inlet pressure			Final average production data								Final permeate production				
																Average data				
TDS %	Inlet m^3/h	R1 %	R2 %	R3 %	S1 bar	S2 bar	S3 bar	Flux lmh	Flow m^3/h	TDS ppm	REC %	Energy kWh/m^3	CCD MR %	PFD MR %	CCD cycles no.	REC %	m^3/h	lmh	ppm	kWh/m^3
0.20	43.7	40	40	40	7.2	9.9	13.9	20.0	34.3	37.6	78.4	0.706	65	0	2	78.8	36.4	21.3	42	0.386
0.20	43.7	45	45	45	7.9	10.5	14.8	21.3	36.4	40.9	83.4	0.654	65	0	3	84.8	38.6	22.5	52	0.406
0.20	43.7	50	50	50	8.5	11.1	16.4	22.3	38.2	46.1	87.5	0.625	65	0	4	88.1	39.7	23.2	62	0.429
0.20	43.7	55	50	50	9.2	11.1	17.0	22.6	38.8	50.2	88.8	0.608	65	0	5	90.3	40.5	23.6	72	0.454
0.20	43.7	60	55	50	10.0	12.2	18.8	23.2	39.8	58.4	91.0	0.602	65	0	6	91.8	41.0	23.9	82	0.479
0.20	43.7	65	55	50	10.8	12.5	20.3	23.5	40.3	65.5	92.1	0.606	65	0	7	92.9	41.3	24.1	93	0.505
0.20	43.7	65	60	50	10.8	13.7	22.0	23.7	40.6	70.0	93.0	0.612	65	0	8	93.7	41.6	24.3	103	0.531
0.20	43.7	65	65	50	10.8	15.1	24.3	23.9	41.0	76.0	93.9	0.622	65	0	9	94.4	41.8	24.4	113	0.557
0.20	43.7	65	65	55	10.8	15.1	26.4	24.1	41.3	78.1	94.5	0.628	65	0	10	94.9	42.0	24.5	123	0.583
0.20	43.7	65	65	60	10.8	15.1	29.0	24.3	41.6	80.8	95.1	0.637	65	0	11	95.3	42.2	24.6	134	0.609
0.20	43.7	65	65	65	10.8	15.1	32.4	24.4	41.8	84.4	95.7	0.648	65	0	12	95.7	42.3	24.7	144	0.636
								23.0										23.7		

the entire process. The average TDS of permeates in the summary takes account of the TDS and flow rates encountered during the stages and the average flux term in the summary is derived from the combined flow rates of permeates and the membrane surface area of the entire design.

The relevant comparative data for the 7ME6 BWRO-CCD unit is derived from Table 3 with or without adjustments of flux and/or PFD recovery in the data base according to the objectives of the analysis. The average flux of BWRO-CCD for comparison with the conventional technique pertains to the average permeate production rate at a given sequence recovery which incorporates the contribution of the initial PFD step in the process. For instance, the average flux during cycle number five of 90.5% recovery in Table 3 corresponds to average permeate flow rate of 40.0 m^3/h and translates to an overall average flux of 23.3 lmh as compared with the fixed flux of 25.0 lmh assumed during the CCD cycles.

The theoretical driven data of the conventional 4ME6-2ME6-ME6 and 7ME6 BWRO-CCD systems provided in Table 6 and the comparative results displayed in Fig. 12(A–C) clearly demonstrate that the latter technique may proceed to any desired recovery without need for staged pressure vessels and interstage booster pumps by an energy saving process (Fig. 12(A)) which yields permeates of somewhat higher TDS (Fig. 12(B)) under similar flux conditions (Fig. 12(C)). A similar comparison is provided in Table 7 and Fig. 13(A–C) for BWR-CCD, wherein PFD-MR = 0%.

The desalination of water sources by conventional BWRO techniques should normally proceed with average flux compatible with the nature of the source with declined flux concomitant with increased fouling factors and/or decreased feed quality and in this context the selected average flux range of 23.0–28.0 lmh in the comparison under review is considered none aggressive for most BRWO applications including such for surface brackish water with MF/UF pretreatment. Most (>90%) common BWRO applications cover the recovery range up to 90% with only few applications requiring higher recovery one of which relates to second-pass desalination of SWRO permeates for boron reduction especially when such a water source also applies for irrigation. Accordingly, special attention in the comparative model analysis under review should be placed on the 75%-90% recovery range wherein most common BWRO applications are being practiced.

Both compared conventional and BWRO-CCD techniques under review involve staged flow and pressure boosted processes; however, these effects are created by different means such as staged pressure

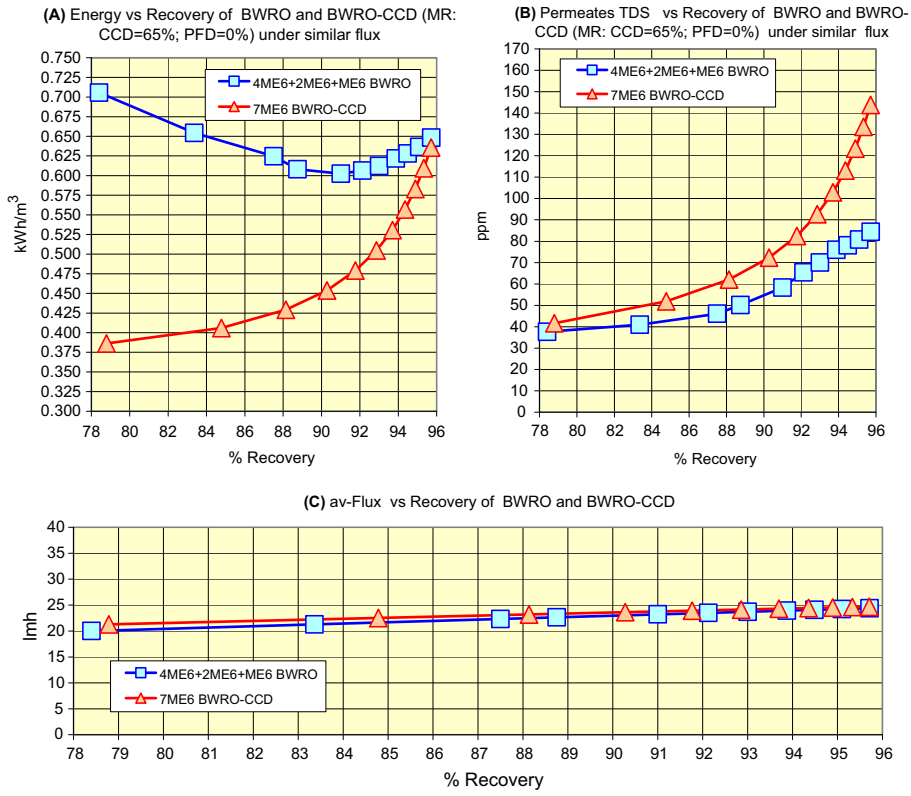

Fig. 13. Energy consumption (A), TDS of permeates (B) and average flux (C) as function of recovery for conventional BWRO and BWRO-CCD according to the data in Table 7.

vessels and inter-stage booster pumps in the former technique; whereas, in the latter technique this is done by mixing of recycled concentrate with pressurized fresh feed at inlet to modules under variable pressure conditions with both flow and pressure compensated without need of staged pressure vessels and inter-stage boosters. The conceptually different operational principles imply that stages in the conventional approach are separately controlled and independent of each other; whereas, in the BWRO-CCD approach the sequential cycles are interconnected and could not be separated from each other. In simple terms, the conventional techniques allow the production of most (50–65%) permeates in the first stage with decreased supplements in the second and third stages, respectively; whereas this is not possible with BWRO-CCD. The performance differences between the techniques under review with respect to energy consumption and salts rejection may be assessed further in light of the theoretical model analysis results as follows:

6.1. Energy consumption aspects

RO desalination is a pressure dependent process with applied pressure expressed by Eq. (3) in terms of flux, average osmotic pressures ($\Delta\pi_{av}$) and pressure difference in modules (Δp). The applied pressure in conventional 3-stage BWRO techniques is controlled by flux at each stage separately with osmotic pressure of subsequent feed determined by the brine effluent of the preceding stage. Power consumption of 3-stage conventional BWRO is therefore a function of declined pressurized feed flow combined with increased pressure boosting along a confined number of stages to the desired recovery. Accordingly, the power requirements of conventional 3-stage BWRO processes manifest the relative contribution of each of the separate stages in the process and their dependence on each other only relates subsequent feed salinity and pressure boosting which are separately controlled. In contrast with the staged flow and pressure boosted conventional plug flow RO techniques, BWRO-CCD relates to a sequential batch type RO desalination process with recycled concentrates mixed with fresh pressurized feed at inlets to modules and recovery determined by the number of CCD cycles irrespective of the number of elements per module. Batch sequence RO implies negligible brine energy loss since replacement of brine by fresh feed may take place at near atmospheric without desalination or alternatively,

Table 8
Performance comparison between a conventional BWRO system (4ME6+2ME6+ME6) and a 7ME6 BWRO-CCD unit with PFD-MR = 0% of the same number and type of elements (E = ESPA2-MAX) with the same feed source (2,000 ppm NaCl) at 25°C under similar recovery with higher flux for the latter technique

4ME6+2ME6+ME6 (ESPA2-MAX) conventional BWRO design												7ME6 (ESPA2-MAX) CCD–MR = 65% PFD-MR = 0%								
Feed		Recovery			Inlet pressure			Final average production data							Final permeate production					
															Average data					
TDS %	Inlet m^3/h	R1 %	R2 %	R3 %	S1 bar	S2 bar	S3 bar	Flux lmh	Flow m^3/h	TDS ppm	REC %	Energy kWh/m^3	CCD MR %	PFD MR %	CCD cycles no.	REC %	m^3/h	lmh	ppm	kWh/m^3
0.20	43.7	40	40	40	7.2	9.9	13.9	20.0	34.3	37.6	78.4	0.706	65	0	2	78.8	42.9	25.0	35	0.440
0.20	43.7	45	45	45	7.9	10.5	14.8	21.3	36.4	40.9	83.4	0.654	65	0	3	84.8	45.4	26.5	44	0.459
0.20	43.7	50	50	50	8.5	11.1	16.4	22.3	38.2	46.1	87.5	0.625	65	0	4	88.1	46.7	27.3	53	0.482
0.20	43.7	55	50	50	9.2	11.1	17.0	22.6	38.8	50.2	88.8	0.608	65	0	5	90.3	47.6	27.8	61	0.506
0.20	43.7	60	55	50	10.0	12.2	18.8	23.2	39.8	58.4	91.0	0.602	65	0	6	91.8	48.2	28.1	70	0.531
0.20	43.7	65	55	50	10.8	12.5	20.3	23.5	40.3	65.5	92.1	0.606	65	0	7	92.9	48.6	28.4	79	0.557
0.20	43.7	65	60	50	10.8	13.7	22.0	23.7	40.6	70.0	93.0	0.612	65	0	8	93.7	49.0	28.6	87	0.583
0.20	43.7	65	65	50	10.8	15.1	24.3	23.9	41.0	76.0	93.9	0.622	65	0	9	94.4	49.2	28.7	96	0.609
0.20	43.7	65	65	55	10.8	15.1	26.4	24.1	41.3	78.1	94.5	0.628	65	0	10	94.9	49.4	28.8	105	0.635
0.20	43.7	65	65	60	10.8	15.1	29.0	24.3	41.6	80.8	95.1	0.637	65	0	11	95.3	49.6	29.0	113	0.661
0.20	43.7	65	65	65	10.8	15.1	32.4	24.4	41.8	84.4	95.7	0.648	65	0	12	95.7	49.8	29.0	122	0.687
								23.0										27.9		

at a somewhat elevated pressure with low desalination recovery and considerable energy saving. The low power consumption pathway offered by BWRO-CCD manifests increased sequence recovery concomitance with increased number of CCD cycles of strong feed dilution effect which translate to a parabolic exponential power consumption curve with actual consumed power represented by its average. Under the fixed flow and variable conditions of the BWRO-CDD process, the overall specific energy is expressed by Eq. (17); wherein, the major contribution (~90%) relates to the average applied pressure (p_{av}) requirements of HP (Eq. (16)) and the minor contribution (Eq. (15)) to the cross-flow (Q_{CP}) and the pressure supplement (Δp) requirements of the CP.

The comparative specific energy requirements on the basis of a theoretical model analysis of a conventional 3-stage system (4ME6-2ME6-ME6) and the equivalent 7ME6 BWRO-CCD unit of the same number of modules (7) and elements (42) of the same type (ESPA2-MX) with the same feed source (2,000 ppm NaCl) are illustrated in Figs. 12–14 and explained hereafter. The energy consumption of the compared systems under similar conditions of flux and recovery is displayed in Fig. 12(A) reveals large gap in favour of the BWRO-CCD when operated according to the data base in Fig. 3 with PFD-MR = 20% and the gap increases according to Fig. 13(A) when the step in the process of brine replacement by fresh feed takes place without desalination (PFD-MR = 0%). The energy saving advantages of BWRO-CCD over conventional BWRO techniques are pronounced in particular in the common 80–90% recovery range of most practiced BWRO applications. The decreased energy consumption gap with increased recovery revealed in Figs. 12(A) and 13(A) manifests the effectiveness of BWRO-CCD in reduction of brine effluent energy losses without need of energy recovery means especially under ≤ 90% recovery. The specific energy data furnished in Fig. 14(A) pertains to the simulated conditions in Table 8 of BWRO-CCD performance with PFD-MR = 0% under higher average flux (27.9 instead 23.0 lmh) compared with the conventional technique and the data reveals the energy saving preference of BWRO-CCD even under increased flux conditions, although the energy gap in the 80–90% recovery range become somewhat smaller as expected by theory.

The aforementioned theoretical BWRO model analysis of the 7ME6 assembly in its conventional staged form (e.g. 4ME6-2ME6-ME6) or its none conventional CCD form should yield similar comparative results for any such general assembly type NMEn of same number of modules (*N*) and elements per module (*n*)

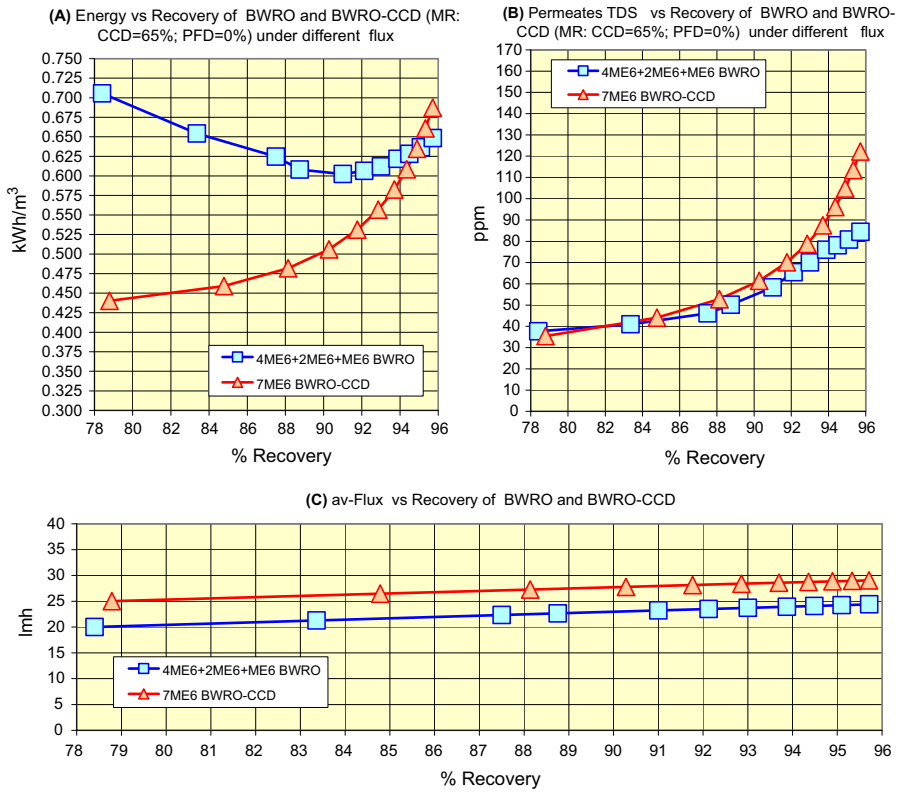

Fig. 14. Energy consumption (A), TDS of permeates (B) and average flux (C) as function of recovery for conventional BWRO and BWRO-CCD according to the data in Table 8.

which show the energy saving preference by BWRO-CCD compared with conventional techniques.

6.2. Permeates quality aspects

Salt rejection of elements with the same diffusion coefficient (*B*) depends according to Eq. (10) on the feed concentration, flux and average concentration polarization factor with the latter according to Eq. (2) being a function of the average element recovery term in Eq. (1). The average TDS of permeates derived from the theoretical model analysis the 3-stage conventional BWRO system (Fig. 1) and the BWRO-CCD unit (Fig. 2) of the same number of modules and elements are compared in Figs. 12(B), 13(B) and 14(B) as function of flux, CCD inlet feed concentration and recovery. The BWRO-CCD sequence comprises a brief initial PFD step of brine replacement by fresh feed followed by CCD cycles to the desired recovery level. The PFD step may take place with or without desalination and the compared data in Figs. 12(B) and 13(B) pertains to cases of PFD-MR = 20 and 0%, respectively.

The separation of the conventional techniques into three distinct stages of decreased feed flow of increased salinity enables to get up to 65% of the permeates under the preferred conditions of low TDS in the first stage with lesser quality permeates received with declined flow rate during the second and third stages, respectively. In contrast, separation between CCD cycles in BWRO-CCD is not possible; however, in this case a dilution effect does take place which moderates inlet feed concentrations to modules by mixing with fresh feed and thereby, causing improved quality permeates. Assessment on the basis of the aforementioned may suggest somewhat improved quality permeate by the conventional three-stage process compared with BWRO-CCD in the 80–90% recovery range under the same average flux conditions with the same initial feed and final brine concentrations at the same overall recovery.

The comparative TDS of permeates in Fig. 12(B) on the basis of the data in Table 6 reveals permeates of ~38(50) ppm at 80% recovery and ~55(78) ppm at 90% recovery under similar flux conditions with the inferior data in parentheses pertaining to BWRO-CCD. However, the compared data pertains to 2,000 ppm NaCl feed at inlet to the first stage of the conventional technique and 2,500 ppm NaCl at the start of the CCD cycles in BWRO-CCD (Table 3) due to the preliminary PFD step of 20% recovery. In simple terms, the major

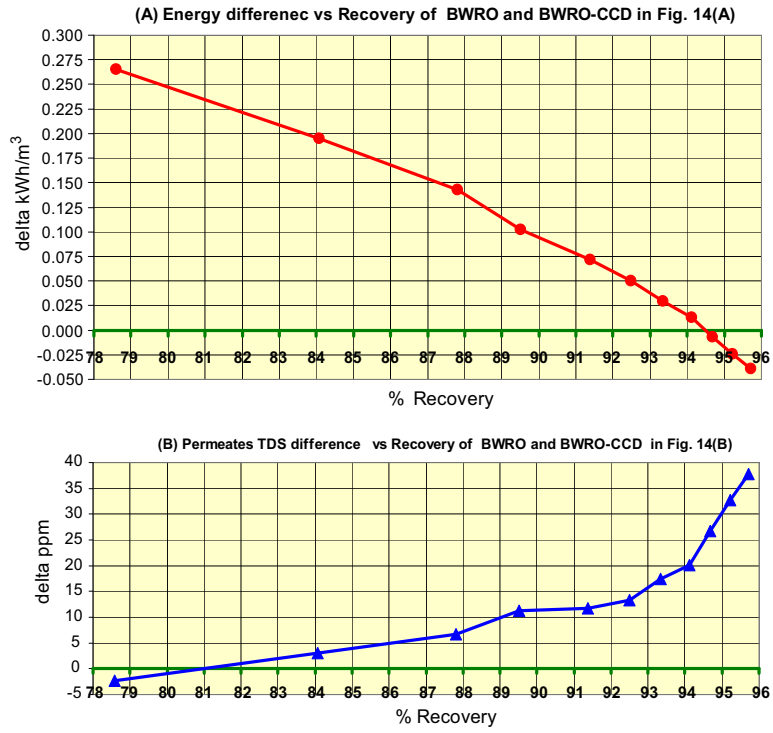

Fig. 15. Differences energy (A) and TDS of permeates (B) as function of average recovery of 3-stage conventional BWRO compared with BWRO-CCD according to the data in Table 8.

part of the TDS difference can be attributed to feed salinity differences. In order to overcome the feed salinity difference, the comparative TDS of permeates described in Fig. 13(B) on the basis of the data in Table 7 pertains to zero desalination during the PFD step of the BWRO-CCD (PFD-MR = 0%) process and this comparison reveals permeates of ~38(40) ppm at 80% recovery and ~55(70) ppm at 90% recovery under similar flux conditions with the inferior data in parentheses pertaining to BWRO-CCD. The improved results in Fig. 13(B) reveal a smaller gap in TDS of permeates (ΔS) at 80% recovery (ΔS = ~2 ppm) which increases with recovery (e.g. REC = 85%, ΔS = ~10 ppm; REC = 90%, ΔS = ~15 ppm and REC = 93%, ΔS = ~22 ppm). The inevitable conclusion reached on the basis of aforementioned analysis is that increased recovery with increased number of CCD cycles invariable leads to permeates of inferior TDS quality compared with the 3-stage conventional approach whereby most permeates are product in the first stage.

6.3. Energy consumption and permeate quality aspects

Energy consumption and salt rejection are effected by flux in opposite directions and therefore, it was found to be of interest to ascertain the flux conditions under which permeates TDS of both techniques are about the same and their effect on energy consumption. The comparative data described in Table 8 pertains to zero desalination during the PFD step of a BWRO-CCD (PFD-MR = 0%) process performed with fixed CCD flux (30 lmh) and the results under such conditions as function of recovery are displayed in Fig. 14(A) for specific energy consumption, in Fig. 14(B) for TDS of permeates and in Fig. 14(C) for average operational flux. Noteworthy in Fig. 14 is the near TDS average of permeates received with distinctly lower energy consumption over the 80–90% recovery range by BWRO-CCD by just ~5.0 lmh raise of flux. Accordingly, for most common water treatment applications in the 80–90% recovery range the BWRO-CCD technique may offer permeates of similar quality to convention techniques with distinct savings of energy under flexible operational conditions of low fouling characteristics. The aforementioned may also suggest the obtainment of improved quality permeate by BWRO-CCD compared with conventional techniques at the same energy consumption level of both.

The differences encountered in Fig. 14(A–B) between the compared techniques are displayed in

Fig. 15(A) and (B) with respect to specific energy (A) and TDS of permeates (B). The results in Fig. 15 with respects to both energy and permeates TDS reveal near linear relationships in the recovery range 78–88% and the development of parabolic exponential relationships thereafter (>88%). The aforementioned observations most probably imply similar near linear effects during the first 2 stages of the conventional techniques and the first 4 CCD cycles of BWRO-CCD, since such near linear effects will generate near linear differences.

7. Concluding remarks

Some aspects of the newly emerging BWRO-CCD technology described hereinabove reveal the plausible application of ME4 (MR = 40–50%), ME5 (MR = 40–60%) and ME6 (MR = 40–65%) modules in the indicated MR ranges (in parentheses) in the context of this technology. A comprehensive theoretical model analysis performed on the conventional 4ME6-2ME5-ME6 system compared with the 7ME6 BWRO-CCD unit design of the same number of modules and elements (ESPA2-MAX) under similar or different flux and recovery conditions described and discussed hereinabove led to several noteworthy conclusions as follows:

(1) BWRO-CCD may reach any desired high recovery made possible by the composition and quality of the source without need of staged pressure vessels and booster pumps and with greater facility and flexibility compared with conventional techniques.
(2) The energy consumption of BWRO-CCD is considerably lower compared with that of conventional techniques under same flux conditions, especially in the 80–90% recovery range, without any need or energy recovery.
(3) The quality of BWRO-CCD permeates in the 80–90% recovery range is somewhat inferior to that of conventional techniques under the same flux conditions.
(4) BWRO-CCD flux increase of ~25% compared with that of conventional techniques will lead to similar quality permeates in the 80–90% recovery range with lower energy consumption by the former despite the raised flux.
(5) Conventional multi-stage BWRO techniques require high MR in the first stage (up to ~65%) in order to reach high ultimate process recovery and this implies increased probability of fouling and scaling of tail elements due to decreased average cross-flow; whereas, MR in BWRO-CCD is independent of sequence recovery and this enables MR selection of desired cross-flow to minimize fouling and scaling effects.

Acknowledgements

Funds to Desalitech Ltd. by AQUAGRO FUND L.P. (Israel) and by Liberation Capital LLC (USA) are gratefully acknowledged.

References

[1] M. Elimelech, W.A. Phillip, The future of seawater desalination: Energy, technology, and the environment, Science 333 (2011) 712–717.
[2] N. Voutchkov, Membrane seawater desalination—overview and recent trends, IDA Conference, November 2–3, 2010, Huntington Beach, CA, USA.
[3] N. Voutchkov, R. Semiat, Seawater desalination, in: N. Li, A.G. Fane, W.S. Ho, T. Matsuura (Eds), Advance Membrane Technology and Applications, John Wiley, Hoboken, NJ, 2008, pp. 47–86.
[4] L.F. Greenlee, D.F. Lawler, B.D. Freeman, B. Marrot, P. Moulin, Reverse osmosis desalination: Water sources, technology, and today's challenges, Water Res. 43 (2009) 2317–2348.
[5] Waterlines Report Series No 9, October 2008, Emerging trend in desalination: A review, UNESCO Centre for Membrane Science and Technology, University of New South Wales, Commissioned by the National Water Commission, Australian Government.
[6] B. Pangarkar, M.G. Sane, M. Guddad, Reverse osmosis and membrane distillation for desalination of groundwater: A review, ISRN Mat. Sci., 2011, Article ID 523124, 9 pages, doi: 10.5402/2011/523124.
[7] J.P. MacHarg, Principle Investigator, Energy Optimization of Brackish Groundwater Reverse Osmosis Desalination, Final Report for Contract Number 0804830845, Texas Water Development Board, Austin, TX 78711-3231, September 2011.
[8] P. Zhang, J. Hu, W. Li, H. Qi, Research progress of brackish water desalination by reverse osmosis, J. Water Res. Prot. 5 (2013) 304–309.
[9] Dow Liquid Separation, FILMTEC™ Reverse Osmosis Membranes, Technical Manual as an example.
[10] A. Efraty, R.N. Barak, Z. Gal, Closed circuit desalination—A new low energy high recovery technology without energy recovery, Desalin. Water Treat. 31 (2011) 95–101.
[11] A. Efraty, R.N. Barak, Z. Gal, Closed circuit desalination series no-2: New affordable technology for sea water desalination of low energy and high flux using short modules without need of energy recovery, Desalin. Water Treat. 42 (2012) 189–196.
[12] A. Efraty, Closed circuit desalination series no-6: Conventional RO compared with the conceptually different new closed circuit desalination technology, Desalin. Water Treat. 41 (2012) 279–295.
[13] A. Efraty, Closed circuit desalination series no-8: Record saving of RO energy by SWRO-CCD without need of energy recovery, Desalin. Water Treat. (in press).

[14] R.L. Stover, N. Efraty, Low energy consumption with closed circuit desalination, Desalin. Water Reuse 4(3) (2012) 12–19.
[15] A. Efraty, Closed circuit desalination series no-3: High recovery low energy desalination of brackish water by a new two-mode consecutive sequential method, Desalin. Water Treat. 42 (2012) 256–261.
[16] A. Efraty, Closed circuit desalination series no-4: High recovery low energy desalination of brackish water by a new single stage method without any loss of brine energy, Desalin. Water Treat. 42 (2012) 262–268.
[17] A. Efraty, Z. Gal, Closed circuit desalination series no 7: Retrofit design for improved performance of conventional BWRO system, Desalin. Water Treat. 41 (2012) 301–307.
[18] A. Efraty, J. Septon, Closed circuit desalination series no-5: High recovery, reduced fouling and low energy nitrate decontamination by a cost-effective BWRO-CCD method, Desalin. Water Treat. 49 (2012) 384–389.
[19] R.L. Stover, Industrial and brackish water treatment with closed circuit reverse osmosis, Desalin. Water Treat. 51 (2013) 1124–1130.
[20] A. Efraty, Apparatus for continuous closed circuit desalination under variable pressure with a single container, US Patent No. 7,628,921 and related patents issued worldwide.
[21] A Efarty, Continuous closed-circuit desalination apparatus without containers, US Patent No. 7,695,614 and related patents issued worldwide.